C.P. No. 414
(20,474)
A.R.C. Technical Report

C.P. No. 414
(20,474)
A.R.C. Technical Report

MINISTRY OF SUPPLY

AERONAUTICAL RESEARCH COUNCIL

CURRENT PAPERS

Static and Dynamic Response of a Design of Differential Pressure Yawmeter at Supersonic Speeds

by

L. J. Beecham, B.Sc.(Eng.)

S. J. Collins, A.M.I.Mech.E.

LONDON: HER MAJESTY'S STATIONERY OFFICE

1958

PRICE 7s. 6d. NET

C.P. No.414

U.D.C. No. 533.6.054:533.6.083.2:533.6.013.154:533.665.011.5

Report No. G.W.19

February, 1954

ROYAL AIRCRAFT ESTABLISHMENT

Static and Dynamic Response of a Design of Differential Pressure Yawmeter at Supersonic Speeds

by

L. J. Beecham, B.Sc.(Eng.)
and
S. J. Collins, A.M.I.Mech.E.

SUMMARY

Static calibration curves are provided for incidences up to 30° at speeds from M = 1.3 to 1.9, and the instrument is shown to resolve accurately when rolled out of the free stream incidence plane. Relations are developed from which a close approximation to the Mach No., incidence and roll angle may be obtained, without recourse to calibration curves, in terms of the differential pressures across each pair of holes and the pitot pressure measured at an axial hole; the free stream static pressure requires to be determined independently.

The dynamic behaviour of the instrument and associated pressure pick-ups is examined, and a design developed for which the acoustic natural frequency is high compared with that likely to be encountered in flight. Certain inconsistencies have been observed between the characteristics as determined separately from the response to a pressure pulse in still air and that from an incidence cycle in a supersonic air stream, and it is suggested that these arise from changes in flow conditions within the tubes under lateral accelerations.

LIST OF CONTENTS

		Page
List of Symbols		4
1	Introduction	7
2	Test equipment	8
3	Static response	9
	3.1 Calibration of pressure difference variation with incidence	9
	3.2 Discrepancy between present results and those of ref.3	10
	3.3 Resolution with roll angle	11
	3.4 Pitot and static pressure measurements	11
	3.5 Determination of incidence, roll angle and Mach No. from flight records	12
4	Dynamic tests	16
	4.1 Response equation	16
	4.2 Theoretical acoustic characteristics at supersonic speeds	22
	4.3 Measurement technique	23
	4.4 Tests and results	24
	4.5 Discrepancy between the response in still and supersonic air	27
	4.6 Further development	29
5	Conclusions	29
References		31

LIST OF APPENDICES

	Appendix
Effect of inaccurate pressure hole location	I
Condition that $2\bar{Z}_1 \bar{Z}_3 << \bar{Z}_2 (\bar{Z}_1 + \bar{Z}_3)$	II
An example of the data extraction methods of para.3.5	III

LIST OF ILLUSTRATIONS

	Fig.
Details of yawmeter head	1
Calibration curves of differential pressure versus incidence	2
Variation of sensitivity with Mach No.	3
Variation of differential pressure with roll angle	4
Resolution in pitch and yaw	5
Variation of pitot pressure with incidence	6
Recorded static pressure variation with incidence (M = 1.4)	7
Relation between Mach No. and p_o/p_s	8
Charts for the determination of θ and M in terms of the pitot pressure and the differential pressure in the combined plane	9
Electrical analogue of yawmeter and pick-up system	10
Relations between acoustic damping and u.n.f. in flight and wind tunnel and that in still air	11
Dynamic test equipment	12
Pressure pick-ups	13
Yawmeter with built-in capacity type pick-up	14
Pressure response of yawmeter with bellows pressure recorder	15
Pressure response of yawmeter with built-in capacity pick-up to an impulse in still air	16
Response of built-in version to mechanical vibration	17
Time lag of interim (long tube) version programmed $\pm 15^\circ$ at 3 c.p.s. (M = 1.9)	18
Steady state pressure response at fast programme speeds (capacity type pick-up)	19
Pressure difference due to an independent (subsonic) cross flow velocity	20
Geometric relations between indicated and true incidence and roll angle	21

LIST OF SYMBOLS

a	speed of sound
A_1	tube cross-sectional area
A_2	chamber cross-sectional area
C_1	acoustic capacitance of the pick-up chamber
C_2	acoustic equivalent of the diaphragm compliance
d.n.f.	damped natural frequency
$g(S)$	initial condition functions
$G(S)$	
i	acoustic equivalent of electrical current
k	$\left[\left\{(\mu_2 - \mu_1)^2 + (n_1 - n_2)^2\right\}\left\{(\mu_2 - \mu_1)^2 + (n_1 + n_2)^2\right\}\right]^{\frac{1}{2}}$
$K(M)$	$\left[\dfrac{\partial\left(\dfrac{\Delta p}{p_s}\right)}{\partial(\sin 2\theta)}\right]$
ℓ	length of connecting tube between pressure holes and pick-up
L_1	acoustic inductance of the air in the pressure tubes
L_2	acoustic equivalent of the diaphragm mass
m_1	air mass in each pressure tube
m_2	mass of pick-up diaphragm and moving parts
M	free stream Mach No.
n_1	$2\pi \times$ acoustic d.n.f. $= (\omega_1^2 - \mu_1^2)^{\frac{1}{2}}$
n_2	$2\pi \times$ mechanical d.n.f. $= (\omega_2^2 - \mu_2^2)^{\frac{1}{2}}$
p	pressure on hemisphere surface
p_o	stagnation pressure (<u>behind</u> normal shock at supersonic speeds)
p_{pit}	pressure registered at axial pitot hole
p_s	free stream static pressure
Δp_1	differential pressure between holes forming roll datum
Δp_2	differential pressure between holes normal to roll datum
Δp	differential pressure in the combined (θ) plane

LIST OF SYMBOLS (CONTD)

q	$\frac{1}{2}\rho_s U^2$
Q	pick-up chamber volume
r	radius of connecting pressure tubes
r_1	$\frac{\omega}{\omega_1}$
r_2	$\frac{\omega}{\omega_2}$
R	distance from inlet holes to the instantaneous centre of rotation
R_s	radius of hemispherical head
R_1	acoustic resistance of pressure lines
R_2	acoustic equivalent of the diaphragm mechanical resistance
S	Laplace transform parameter
t	time variable
u.n.f.	undamped natural frequency
U	free stream velocity
v	pressure registered by pick-up
V	pressure at yawmeter inlet holes
V_o	input pressure amplitude
Z_1, Z_2, Z_3	equivalent acoustic impedances
$\overline{Z}_1$	$L_1 S + R_1$
$\overline{Z}_2$	$L_2 S + R_2 + \frac{1}{C_2 S}$
$\overline{Z}_3$	$\frac{1}{C_1 S}$
α_1	incidence in plane of holes forming roll datum
α_2	incidence normal to plane of holes forming roll datum
ε	phase angle
ζ_1	acoustic damping factor $= \frac{\mu_1}{\omega_1}$
ζ_2	mechanical damping factor $= \frac{\mu_2}{\omega_2}$

LIST OF SYMBOLS (CONTD)

η	dynamic viscosity of air in pressure lines
θ	incidence of yawmeter axis to the free stream
θ_o	nominal angular location of pressure holes relative to yawmeter axis
θ_{o1}, θ_{o2} etc	actual location of individual holes
μ_1	$\frac{R_1}{2L_1}$
μ_2	$\frac{R_2}{2L_2}$
ρ_s	air density in free stream
ρ	air density in pressure line
τ	time lag
ϕ	roll angle
ψ	$\theta + \theta_o$
ω	$2\pi \times$ forcing frequency
ω_1	$2\pi \times$ acoustic u.n.f.
ω_2	$2\pi \times$ mechanical u.n.f.

Superscripts

$\cdot$	$\frac{d}{dt}$
$-$	Laplace operator form $\left(\text{i.e. } \overline{V} = \int_o^\infty V e^{-st}\, dt\right)$

Other suffices

E	manufacturing error
F	in flight conditions
I	indicated
T	in wind tunnel conditions

1 Introduction

Until fairly recently no direct measurement of the incidence of a body or surface to the free stream direction had been made in the course of supersonic missile flight trials carried out in this country. In the R.A.E./G.W. Dept. tests the steady state (trim) incidence has in the past been obtained in a roundabout way during the determination of the aerodynamic pitch derivatives from the normal acceleration, response frequency and damping of a programmed test vehicle. The derivatives so obtained refer to small perturbations about the steady state conditions, and generally one round has provided information at one incidence only. With linear aerodynamics two rounds are required to furnish all the required data at one incidence; in practice the derivatives are often non-linear with incidence and several more rounds are necessary to provide a complete picture.

This method is costly in rounds as well as being sensitive to round-to-round asymmetries, and some direct means of determining the attitude of the missile or its surfaces to the free stream direction is obviously desirable. An incidence measuring instrument of even a slow response would be sufficient to measure the trim angle· an instrument with a response frequency high enough to record the instantaneous incidence during a transient motion would decrease very considerably the firings needed to produce the same data as in the past.

The types of instrument suitable for this purpose fall into two principal classes, viz.

(i) those in which the incidence is registered directly as the angle turned through by a surface in aligning itself along the local stream direction (the surface may have one or more degrees of freedom), and

(ii) those which remain fixed in missile axes, and whose function depends upon the extent of the flow changes induced by incidence.

An example of the former is the low aspect ratio delta wing vane of which several designs with freedom in one, and latterly two, planes are now available. These have the merit of recording the flow inclination, which, providing interference from the missile is avoided, gives the incidence directly. However they have at present a limited range of angle, and it has not yet been established that with one degree of freedom they will resolve correctly when the motion of the vane relative to the missile is not in the pitch plane.

The principal example of the other class is the differential pressure yawmeter*, and it is with this type that this report is concerned. A number of designs are available utilising the pressure differences set up between pairs of holes in the instrument when at incidence. In this way the pressure difference may be registered in any plane by appropriately positioning the holes; in general for a cruciform missile two pairs only, with their joins perpendicular, are required and it is probable that these would be aligned so as to record normally to the wing planes.

---

*The term "yawmeter" is used throughout to describe an instrument measuring incidence in any plane.

This type of instrument has the disadvantage that the sensitivity, i.e. the pressure difference per degree of incidence, is dependent on both Mach No. and the ambient atmospheric pressure in flight. This may require a pressure pick-up sensitive over a wide range when the missile is to be flown in widely varying speed and altitude conditions. As far as the reduction of the data is concerned the dependence on ambient pressure need present little difficulty. Under flight trial conditions the ambient air pressure is always deducible from trajectory and meteorological information, and it is not unlikely that methods can be developed to measure it by pick-ups in the missile itself. The Mach No. can conveniently be determined by measurement of the supersonic pitot pressure in conjunction with the static (ambient) air pressure, and this can be obtained either from a separate instrument, or, as will be shown, by a suitable pressure hole in the yawmeter head. Although less direct in operation this instrument has some advantages over the vane type. It has, for instance, a much larger potential incidence range since there are no mechanical limitations, and it has already been shown to resolve the component angles satisfactorily at incidences up to 10°. It has a further advantage that the pick-ups are interchangeable, and thus the sensitivity can be designed to give the largest signal appropriate to the operating conditions.

The yawmeter examined in the present tests is a design on which a certain amount of static testing has already been done in 19" x $27\frac{1}{2}$" O.A.L. tunnel at Daingerfield, Texas. The present tests examine in more detail the variation of static sensitivity with Mach No. and extend the incidence range up to 30°; roll resolution up to 35° incidence is investigated at one Mach No. In addition to the tests on the basic instrument, for which the angular location, θ_o, of the differential pressure holes relative to the axis is 45°, calibrations are also given for $\theta_o \div 49^{\circ}$ and for $\theta_o \div 53^{\circ}$. As will be shown the empirical laws derived suggest that the maximum sensitivity occurs with $\theta_o \div 54^{\circ}$.

In addition an attempt is made to measure the dynamic response of the instrument and associated recording equipment under still air and supersonic conditions, and to increase the response frequency as far as possible in order to render the instrument capable of registering missile incidence during transient motion.

2 Test equipment

All wind tunnel tests were carried out in the R.A.E. No.18 (9" x 9") supersonic tunnel at atmospheric stagnation pressure. For the static tests pressures were measured on an orthodox mercury manometer. For the dynamic tests pressures were recorded initially on a bellows type pick-up using stylus-on-celluloid recording (fig.13a). Subsequently a capacity type differential pick-up (fig.13b) was used in conjunction with frequency modulated capacity measuring equipment enabling the signal from the pressure pick-up to be displayed as a D.C. voltage on a cathode ray oscilloscope (fig.12). The signal was recorded photographically by means of a Type 1428 Cossor Camera, a suitable time base being injected by a signal generator.

Details of the basic ($\theta_o = 45^{\circ}$) yawmeter head are given in fig.1. Several instruments were constructed in the course of developmental work, and details are given below:-

Ref. No.	Details	θ_o
1	"One-off static version" - also used for first dynamic tests with bellows type pick-up	$48^\circ 52' \pm 28'$
2	"One-off dynamic version" - used for intermediate dynamic tests with the capacity pick-up mounted outside the tunnel. Also used for roll resolution tests	$45^\circ 30' \pm 20'$
3	R.A.E. production version - static tests at supersonic speeds	$44^\circ 42' \pm 2\frac{1}{2}'$
4	De Havilland production version 1 - static tests at supersonic speeds	$52^\circ 48' \pm 30'$
5	De Havilland production version 2 - static tests at transonic speeds	$52^\circ 20' \pm 10'$
6	R.A.E. version with built-in capacity pick-up - dynamic tests only.	

3 Static response

Before the instrument could be used for precise flight test work it was felt that an elaboration of the previous calibrations was desirable. In particular an extension of the calibration incidence range and the production of pressure difference versus incidence curves at smaller Mach No. increments were required, and also it was thought necessary to examine the resolution characteristics of the instrument when the missile incidence plane was not in the plane of one or other pairs of holes. It had previously been verified that up to angles of attack of 10° the instrument resolved correctly and it was necessary to extend the measurement of the deviation (i.e. indicated - actual incidence) up to 30° or more.

3.1 Calibration of pressure difference variation with incidence

For the calibration against angle of incidence the instrument was orientated so as to have nominally zero roll angle, i.e. the plane containing the yawmeter axis and one pair of holes was arranged to coincide as nearly as possible with that in which the instrument was pitched. The incidence datum was taken as that position in which there was no pressure difference between these holes. The effects of small misalignment errors are examined in detail in Appendix I.

At M = 1.3 the incidence obtainable was limited to 25° by tunnel blockage; at all the higher speeds the pressures were measured over an incidence range of 30°.

The yawmeter calibration curves, obtained by differencing the pressures at each incidence, are given in figs.2. The pressures have been non-dimensionalised with reference to the static pressure of the undisturbed stream. These curves show that for incidences up to 10° the yawmeter behaves almost linearly, but at higher angles there is an increasing tendency for the pressure to tail off.

The solution for incompressible flow around a sphere gives the pressure, p, at a point on the surface an angle, ψ, from the stagnation point as

(1)

$$p = p_o - \frac{9}{4}(p_o - p_s)\sin^2\psi \qquad (1)$$

where p_s and p_o are respectively the free stream static and stagnation pressures. If ψ is regarded as consisting of an angle θ_o relative to an axis fixed in the sphere, and an angle θ between this axis and the free stream direction it is readily shown that the pressure difference between two symmetrically disposed holes is

$$\frac{\Delta p}{p_s} = \frac{9}{4}\left(\frac{p_o}{p_s} - 1\right)\sin 2\theta_o \sin 2\theta \qquad (2)$$

giving $$\left(\frac{\Delta p}{p_s}\right)_{max} = \frac{9}{4}\left(\frac{p_o}{p_s} - 1\right)\sin 2\theta \quad \text{for } \theta_o = 45^\circ \qquad (3)$$

Comparison of equation 3 with the experimental curves shows that the non-linearity with θ is prescribed very well by sin 2θ (fig.2), but that the slope, $\dfrac{\partial\left(\frac{\Delta p}{p_s}\right)}{\partial(\sin \partial\theta)}$, differs considerably from $\frac{9}{4}\left(\frac{p_o}{p_s} - 1\right)$ at supersonic speeds (fig.3). It is found, however, (see para.3.5) that the sensitivity is given very closely by a factor of roughly similar form, viz. $K_1\left(\frac{p_o}{p_s} - \frac{1}{2}\right)$, where, at supersonic speeds, p_o is the stagnation pressure behind a normal shock at the relevant Mach No. and K_1 = 0.925 and 0.954 for $\theta_o = 45^\circ$ and 53° respectively. The empirical curves are plotted on fig.3 together with experimental results obtained from the one-off static (No.1) and dynamic test (No.2) instruments, and also for the production versions (Nos.3, 4) made by R.A.E. and De Havilland Propellers Ltd. The effect of differences in angular location of the holes on the hemisphere appears to be small but nevertheless the maximum sensitivity is obtained for a value of θ_o somewhat greater than 45°.

Also included on this figure are preliminary values obtained with No.5 at transonic and high subsonic speeds over a small incidence range ($\pm 4^\circ$) in the N.A.E. 3 ft x 3 ft wind tunnel. This work carried out by N.A.E. Staff, has been reported in detail in reference 2.

3.2 Discrepancy between the present results and those of reference 3

It is apparent from fig.3 that there is a considerable discrepancy between the results of the present calibration and that carried out at Daingerfield with virtually the same instrument as No.3.

The source of this discrepancy is not known. It has been demonstrated that considerable latitude can be given to the location of the holes without much change of sensitivity, so that, on the assumption that the pressure measuring equipment is above suspicion the indication is that the cause lies in profile differences. It points the need for precision manufacture of these instruments if they are to be widely adopted as standard equipment.

3.3 Resolution with roll angle

Tests to examine the ability of the instrument to resolve correctly when the holes are asymmetrically disposed with respect to the pitch plane were carried out at one Mach No. (M = 1.4) only, but it is felt that the results can be applied qualitatively throughout to the speed range of tests in the previous section. Pressures were measured at 15° increments in roll over the range 0 to 90°, and 5° increments in incidence over a range $\pm 35^{\circ}$. For design reasons it was not practicable to use the calibrated instruments Nos.1, 3, 4 for these tests; instead they were carried out with the one-off dynamic test version, No.2, used for the dynamic response tests of section 4.

The differential pressure is shown plotted in fig.4 against roll angle, ϕ, and it is apparent from the curves that there was a roll misalignment error of -2° and a misalignment of the yawmeter and stream axes of 0.3°. These have been corrected for in fig.5 which shows the relation between the known streamwise* incidence, α, (where $\sin \alpha = \sin \theta \cos \phi$) in the plane of the holes and that indicated by the pressure difference between these holes as determined by the values at $\phi = 0$. For correct resolution all the points should be on a single curve; instead they are seen to be on a series of narrow envelope curves, corresponding to constant values of θ, the width of the envelope indicating the extent to which the pressure difference is dependent upon roll angle. Over the range of incidence, θ, from 0 to 35° the maximum deviation of the indicated from the actual incidence in the plane of the pressure holes occurred at roll angles between 40° and 60°. The magnitude is given below:-

Incidence θ°	Deviation as % of actual incidence
0 to 15°	Less than -1%
20°	-1.6
25°	-2.7
30°	-4.2
35°	-7.5

3.4 Pitot and static pressure measurements

Although the present tests are principally concerned with the behaviour of the instrument as a flow angle measuring device it is evident from the foregoing sections that, since the sensitivity is a function of both static pressure and Mach No., additional information is required before the incidence can be deduced from a differential pressure measured during flight. To this end pitot and static holes were provided in the instrument, the former axially disposed on the hemisphere so as to register stagnation pressure at zero incidence, and the latter positioned

*As distinct from the so-called "chordwise" definition, $\tan \alpha = \tan \theta \cos \phi$.

$3\frac{1}{2}$ calibres behind the nose in accordance with the recommendations of reference 3, and arranged as a circumferential ring of 12 equally spaced holes. Tests were carried out to see to what extent the pressures recorded at incidence differed from the known stagnation and static pressures.

The variation of pitot pressure with incidence is shown in fig.6, non-dimensionalised in terms of p_s. It was found by plotting $\frac{p_o}{p_s}$ against $\frac{p_{pit}}{p_s}$ for constant incidence, θ, that $\left(\frac{p_o}{p_s} - \frac{1}{2}\right)$ is proportional to $\left(\frac{p_{pit}}{p_s} - \frac{1}{2}\right)$, the constant of proportionality being given closely by $\sec^{3/2}\theta$

i.e. $$\left(\frac{p_{pit}}{p_s} - \frac{1}{2}\right) = \left(\frac{p_o}{p_s} - \frac{1}{2}\right) \cos^{3/2}\theta \qquad (4)$$

This variation is also shown in fig.6. It is of interest that equation 4 is found to predict very closely indeed the pressure distribution over the whole of the hemisphere, and to collapse a great deal of existing pressure data obtained over a wide range of supersonic speeds.

The static pressures at M = 1.4 as recorded at the holes in the cylindrical body are shown in fig.7, non-dimensionalised again with respect to the true free stream static pressure. These pressures are noticeably dependent on the incidence, the value at 17° being only 72% of that at zero angle. Certain modifications to the size, shape and number of holes were tried, but they effected no significant improvement. It is thought unlikely that an accurate measurement of static pressure will be obtained with this type of instrument where the pressure holes are subject to the influence of the vortices shed from the body of the instrument at incidence.

3.5 Determination of incidence, roll angle and Mach No. from flight records

In the application of this instrument to flight test work the requirement will in general be to derive the angles θ and ϕ in polar axes, or α and β in cartesian axes, together with Mach No., from a knowledge of three pressure ratios, viz. $\frac{\Delta p_1}{p_s}$, $\frac{\Delta p_2}{p_s}$ and $\frac{p_{pit}}{p_s}$ the static pressure, p_s, having been determined independently. This can be done by a tedious, purely iterative process from the curves given in figs.2 to 6, but the labour can be reduced, or eliminated depending upon the accuracy required, by several methods.

Firstly, if the incidence range is small, say less than 10°, then the non-linearities may be disregarded and the parameters evaluated as follows:-

$$\left.\begin{aligned} \frac{p_o}{p_s} &\div \frac{p_{pit}}{p_s} \quad \text{and hence Mach No. from fig.8} \\ \alpha_{1,2} &\div \frac{\Delta p_{1,2}}{p_s} \div \underline{2K(M)} \\ \theta &\div \left[\left(\frac{\Delta p_1}{p_s}\right)^2 + \left(\frac{\Delta p_2}{p_s}\right)^2\right]^{\frac{1}{2}} \div 2K(M) \\ \tan\phi &\div \frac{\Delta p_2}{p_s} \div \frac{\Delta p_1}{p_s} \end{aligned}\right\} \quad (5)$$

Here, as elsewhere in this paper, when the reference wings are in-line with the holes forming the roll datum then α_1 and α_2 correspond respectively to the streamwise incidence and sideslip angles, α and β.

When the incidence is not small, incidence and Mach No. may be derived from the charts shown in fig.9(a) and (b) which have been produced by interpolation, and at the lowest speed by extrapolation of the experimental data. If M is known from independent data then the pitot pressure readings are redundant, although they might possibly be used in conjunction with the Mach No. to provide p_s. Providing the errors in roll resolution are neglected (para.3.3) then the angles α_1 and α_2 may be extracted directly from figs.9(a) to 9(b) by reading off the incidences relevant to the known Mach No., and the ratios $\frac{\Delta p_1}{p_s}$ and $\frac{\Delta p_2}{p_s}$ respectively. θ and ϕ may then be derived from the streamwise incidence definition of para.3.3, viz.

$$\left.\begin{aligned} \sin\alpha_1 &= \sin\theta\cos\phi \\ \sin\alpha_2 &= \sin\theta\sin\phi \end{aligned}\right\}$$

giving

$$\left.\begin{aligned} \tan\phi &= \frac{\sin\alpha_2}{\sin\alpha_1} \\ \sin\theta &= [\sin^2\alpha_1 + \sin^2\alpha_2]^{\frac{1}{2}} \end{aligned}\right\} \quad (6)$$

If M is not known then the pressure difference in the combined plane is required before the Mach No. can be determined. Since this pressure difference is non-linear with incidence and the latter is not known, an approximation is necessary. A convenient form is:-

$$\frac{\Delta p}{p_s} \div \left[\left(\frac{\Delta p_1}{p_s}\right)^2 + \left(\frac{\Delta p_2}{p_s}\right)^2\right]^{\frac{1}{2}} \qquad (7)$$

which amounts to assuming that $\sin^2 2\theta \div \sin^2 2\alpha_1 + \sin^2 2\alpha_2$. The error introduced by this approximation, expressed as a fraction of the correct value is:-

$$\text{Error} = \sec\theta[1 - \sin^2\theta(\cos^4\phi + \sin^4\phi)]^{\frac{1}{2}} - 1 \qquad (8)$$

and the sign is such that the approximation overestimates the pressure difference in the combined plane. The error is zero at $\phi = 0$ and 90°, and a maximum of $(1+\frac{1}{2}\tan^2\theta)^{\frac{1}{2}} - 1$ at $\phi = 45^\circ$; at $\theta = 10^\circ$, 20° and 30° this amounts to 1, 3 and 8% respectively. Using this value of $\frac{\Delta p}{p_s}$ and the measured value of $\frac{p_{pit}}{p_s}$, and entering fig.9 at the appropriate point on the axes gives first approximations to M and θ.

These values will often be within the accuracy limits of the flight pressure data, but where justified, they may be refined further by at least two methods. The first is to adopt the above procedure for a known Mach No., using in this case the first approximation to M, to derive α_1 and α_2, and hence ϕ and θ(equations 6). The second is to evaluate the error given by equation 8 using $\phi \div \tan^{-1}\left(\frac{\Delta p_2}{\Delta p_1}\right)$ and the value of θ from the first approximation. This gives a more accurate value of $\frac{\Delta p}{p_s}$ in the combined plane, and this is then used in conjunction with $\frac{p_{pit}}{p_s}$ to evaluate θ and M afresh from fig.9. For an example of these methods see Appendix III.

Another method likely to be useful in simulator studies, or elsewhere where a functional form is required, can be obtained from a consideration of fig.9, the form of which leads to simple empirical expressions for ϕ and $\frac{p_o}{p_s}$. It is noticeable that the θ-constant lines are straight, and these when produced cut the $\frac{p_{pit}}{p_s}$ axis at 0.5. Moreover the slope is very nearly proportional to θ so that we have the very convenient relationship,

$$\theta \text{ in degrees} \div \frac{k_2 \frac{\Delta p}{p_s}}{\left(\frac{p_{pit}}{p_s} - \frac{1}{2}\right)} \qquad (9)$$

where $k_2 = 30.1$ for $\theta_o = 53^\circ$, and
$= 31$ for $\theta_o = 45^\circ$.

As before $\Delta p \doteq [(\Delta p_1)^2 + (\Delta p_2)^2]^{\frac{1}{2}}$, and α_1 and α_2 may be written for θ, with Δp suitably subscribed. The importance of this result is that at the cost of an extra pressure measurement, $\frac{p_{pit}}{p_s}$, the evaluation of incidence can be achieved without a knowledge of the Mach No.

From 9 we have

$$\left[\frac{\partial\left(\frac{\Delta p}{p_s}\right)}{\partial(\sin 2\theta)}\right]_{\theta=0} = 0.954\left(\frac{p_o}{p_s} - \tfrac{1}{2}\right) \text{ for } \theta_o = 53^\circ, \text{ and}$$

$$= 0.925\left(\frac{p_o}{p_s} - \tfrac{1}{2}\right) \text{ for } \theta_o = 45^\circ \qquad (10)$$

and these empirical functions for the sensitivity are shown on fig.3. They give remarkably good agreement with experiment even at transonic and high subsonic speeds.

The sensitivity may also be derived directly from equation 4 by differencing and differentiating, with $\theta = \pm \theta_o$ viz.

$$\left[\frac{\partial\left(\frac{p}{p_s}\right)}{\partial(\sin 2\theta)}\right]_{\theta=0} = \left(\frac{p_o}{p_s} - \tfrac{1}{2}\right) \cdot \frac{3}{2} \cos^{\frac{1}{2}} \theta_o \sin \theta_o \qquad (11)$$

The factor given by equation 11 is within 3% of that of the appropriate term in equations 10.

It is readily shown from 11 that the sensitivity is a maximum when

$\theta_o = \cos^{-1} \frac{1}{\sqrt{3}}$ i.e. 54.7°.

Derivation of the Mach No. requires the evaluation of $\frac{p_o}{p_s}$, and this can be achieved by elimination of θ between equations 4 and 9. However, since the fall off in p_{pit} with incidence is predominantly a square law variation a good and convenient approximation to $\frac{p_o}{p_s}$ is given by,

$$\frac{p_o}{p_s} \doteq \frac{p_{pit}}{p_s} + \frac{0.22\left(\frac{\Delta p}{p_s}\right)^2}{\left(\frac{p_{pit}}{p_s} - \frac{1}{2}\right)} \qquad (12)$$

where the factor 0.22, applicable to both $\theta_o = 45^o$ and 53^o within the order of approximation, has been obtained by fitting the experimental data.

Roll angle may be determined approximately as $\tan^{-1} \frac{\Delta p_2}{\Delta p_1}$. The maximum error in this approximation, for which it is assumed that $\frac{\sin \alpha_2}{\sin \alpha_1} \div \frac{\sin 2\alpha_2}{\sin 2\alpha_1}$, is not more than 2^o for an incidence of 30^o in the combined plane.

From any of these methods it is possible to derive close approximations to incidence, roll angle and, from $\frac{p_o}{p_s}$, Mach No. (fig.8) directly from a measurement of three pressure ratios, viz. the ratios of the recorded pitot pressure and differential pressures across each pair of holes to the free stream static pressure (local ambient pressure in flight). These approximations can always be refined to any required degree by using them as a first stage in a successive approximation process.

A typical worked example is given in Appendix III to demonstrate these various methods and to indicate the orders of the errors involved.

4 Dynamic tests

The tests under non-steady conditions were designed to measure the response of the yawmeter and its auxiliary recording equipment, and to develop either or both as required to render the instrument suitable for flight test work.

The overall response is governed by both the mechanical and acoustic characteristics of the system, and for minimum phase lag between actual and recorded incidence both the acoustic and mechanical u.n.f. (undamped natural frequency) should be as high as possible in conjunction with suitable damping. It has been pointed out elsewhere that the acoustic u.n.f. of pressure operated instruments incorporating considerable lengths of tubing can often be much lower than the mechanical, and the emphasis therefore has been on obtaining an instrument for which the acoustic frequency is high compared with the missile weathercock frequency, for which 3 c.p.s. is taken here as typical.

4.1 Response equation

The yawmeter and pick-up system is shown diagrammatically as an acoustic-mechanical combination in fig.10(a). The difference in chamber pressures produces a deflection of a diaphragm, which constitutes the mechanical system. By the analogue method of reference 1, the system can be shown to be equivalent to the electrical circuit of fig.10(b) in which

R_1 is the acoustic resistance of the air in the pipes $= \frac{8\ell\eta}{\pi r^4}$

L_1 is the acoustic inductance of the air in the pipes $= \frac{4}{3} \frac{\ell\rho}{\pi r^2}$

C_1 is the acoustic capacitance of the chamber $= \frac{Q}{\rho a^2}$

R_2 is the acoustic equivalent of the diaphragm mechanical resistance

L_2 is the acoustic equivalent of the diaphragm mass

C_2 is the acoustic equivalent of the diaphragm compliance

V is the input voltage equivalent in the acoustic system to the differential pressure.

For convenience consider the generalised circuit of fig.10(c) in which the impedance in each branch of fig.10(b) is denoted by Z with an appropriate subscript (Z is the operator $R + L\frac{d}{dt} + \frac{1}{C}\int_o^t dt$ such that $ZI = RI + L\frac{dI}{dt} + \frac{1}{C}\int_o^t I\,dt$).

The equivalent impedance of the whole circuit, Z_E, is

$$Z_E = \frac{(Z_1 + Z_3)(Z_2Z_1 + Z_2Z_3 + 2Z_1Z_3)}{Z_1Z_2 + Z_2Z_3 + 2Z_1Z_3 + Z_3^2} \qquad (13)$$

The input current, $I, = \frac{V}{Z_E}$ and the current in Z_2,

$$i = \frac{VZ_3}{Z_1Z_2 + Z_2Z_3 + 2Z_1Z_3} \qquad (14)$$

The pressure registered by the pick-up is, by analogy, the voltage, v, across C_2 in fig.10(b), and this is given by

$$v = \frac{1}{C_2}\int i\,dt \qquad (15)$$

Now take the Laplace transforms of 14 and 15, and to avoid confusion with the symbol for pressure denote the Laplace transform symbol by S instead of the more usual p, so that

$$\bar{i} = \int_o^\infty i\,e^{-St}\,dt \quad \text{etc.}$$

Then
$$\bar{I} = \frac{V\bar{Z}_3 + g(S)}{\bar{Z}_1\bar{Z}_2 + \bar{Z}_2\bar{Z}_3 + 2\bar{Z}_1\bar{Z}_3} \qquad (16)$$

where g(S) is a function of the initial conditions only.

and $$\bar{v} = \frac{\bar{i}}{SC_2} = \frac{\overline{VZ_3} + g(S)}{SC_2[\bar{Z}_1\bar{Z}_2 + \bar{Z}_2\bar{Z}_3 + 2\bar{Z}_1\bar{Z}_3]} \qquad (17)$$

In the present case $\bar{Z}_1 = L_1S + R_1$

$$\bar{Z}_2 = L_2S + R_2 + \frac{1}{C_2S}$$

$$\bar{Z}_3 = \frac{1}{C_1S} .$$

Now providing Z_1Z_3 is small compared with $(Z_1 + Z_3)Z_2$ (see Appendix II) then the quartic in the denominator of equation 17 may be replaced approximately by a biquadratic, viz

$$\bar{v} = \frac{\overline{VZ_3} + g(S)}{SC_2(\bar{Z}_1 + \bar{Z}_3)\bar{Z}_2}$$

$$= \frac{\bar{V} + G(S)}{L_1C_1L_2C_2\left[S^2 + \frac{R_1}{L_1}S + \frac{1}{L_1C_1}\right]\left[S^2 + \frac{R_2}{L_2}S + \frac{1}{L_2C_2}\right]}$$

$$= \frac{[\bar{V} + G(S)]\ \omega_1^2\,\omega_2^2}{[(S + \mu_1)^2 + n_1^2]\ [(S + \mu_2)^2 + n_2^2]} \qquad (18)$$

where $\omega_1^2 = \frac{1}{L_1C_1}$ = $2\pi \times$ acoustic u.n.f.

$\omega_2^2 = \frac{1}{L_2C_2}$ = $2\pi \times$ mechanical u.n.f.

$\mu_1 = \frac{R_1}{2L_1}$

$\mu_2 = \frac{R_2}{2L_2}$

$n_1 = \sqrt{\omega_1^2 - \mu_1^2}$ = $2\pi \times$ acoustic damped n.f.

$n_2 = \sqrt{\omega_2^2 - \mu_2^2}$ = $2\pi \times$ mechanical damped n.f.

$$\omega_1^2\omega_2^2 . G(S) = \Big[S^3 v + S^2\{\dot{v} + 2(\mu_1+\mu_2)v\}$$

$$+ S\{\ddot{v} + 2(\mu_1+\mu_2)\dot{v} + (4\mu_1\mu_2 + \omega_1^2 + \omega_2^2)v\} + \dddot{v} + 2(\mu_1+\mu_2)\ddot{v}$$

$$+ (4\mu_1\mu_2 + \omega_1^2 + \omega_2^2)\dot{v} + 2(\mu_1\omega_2^2 + \mu_2\omega_1^2)v\Big]_{t=0}$$

Equation 18 gives in subsidiary equation form the response of the combination for a given input, V.

Response to various input programmes

(i) Step function of pressure, V_o

$$t \leqslant 0, \quad V = \bar{V} = 0, \quad v = \dot{v} = \ddot{v} = \dddot{v} = 0 \quad \therefore \quad G(S) = 0$$

$$t > 0, \quad V = V_o \quad \therefore \quad \bar{V} = \frac{V_o}{S}$$

Substituting for $\bar{V}$ and G(S) in 18 and taking the inverse transform gives

$$v = V_o \left[1 - \frac{\omega_1^2 \omega_2^2}{K} \sum_{i=1,2} \frac{e^{-\mu_1 t} \sin(n_i t - \varepsilon_i)}{\omega_i n_i} \right] \qquad (19)$$

for subcritical damping ($\mu_i < \omega_i$).

where $K = \left[\{(\mu_2 - \mu_1)^2 + (n_1 - n_2)^2\} \{(\mu_2 - \mu_1)^2 + (n_1 + n_2)^2\} \right]^{\frac{1}{2}}$

$$\tan \varepsilon_1 = \frac{2\mu_1 n_1 (\mu_2 - \mu_1) \quad n_1 [(\mu_2 - \mu_1)^2 - n_1^2 + n_2^2]}{\mu_1 [(\mu_2 - \mu_1)^2 - n_1^2 + n_2^2] + 2n_1^2 (\mu_2 - \mu_1)}$$

$$\tan \varepsilon_2 = \frac{2\mu_2 n_2 (\mu_1 - \mu_2) - n_2 [(\mu_1 - \mu_2)^2 - n_2^2 + n_1^2]}{\mu_2 [(\mu_1 - \mu_2)^2 - n_2^2 + n_1^2] + 2n_2^2 (\mu_1 - \mu_2)}$$

For supercritical damping ($\mu_i > \omega_i$), n_i is imaginary and the trigonometrical term is replaced by the hyperbolic equivalent (sin ix = i sinh x).

(ii) Pressure impulse, V_o

$$t < 0 \quad V = \bar{V} = 0 \qquad \therefore \quad G(S) = 0$$

$$t = 0 \quad \lim_{\tau \to 0} \int_o^\tau V dt = V_o$$

$$t > 0 \quad V = 0 \qquad \bar{V} = V_o$$

The value for v is given by the differential of the R.H.S. of equation 19 with respect to t. Thus

$$v = \frac{V_o \omega_1^2 \omega_2^2}{K} \sum_{i=1,2} \frac{e^{-\mu_i t} \sin(n_i t - \varepsilon_i)}{n_i} \quad \text{for subcritical damping} \qquad (20)$$

where

$$\varepsilon_1 = \tan^{-1} \frac{2n_1(\mu_2 - \mu_1)}{(\mu_2 - \mu_1)^2 - n_1^2 + n_2^2}$$

$$\varepsilon_2 = \tan^{-1} \frac{2n_2(\mu_1 - \mu_2)}{(\mu_1 - \mu_2)^2 - n_2^2 + n_1^2}$$

(iii) Sinusoidally varying input

$$V = V_o \sin \omega t$$

$$\overline{V} = \frac{V_o \omega}{S^2 + \omega^2}$$

In this case we are concerned only with the steady state response, and the term G(S), which affects the transient response only, is not required.

Thus

$$v = \frac{V_o \sin(\omega t - \varepsilon)}{\left[\{(1 - r_1^2)^2 + 4(r_1\zeta_1)^2\}\{(1 - r_2^2)^2 + 4(r_2\zeta_2)^2\}\right]^{\frac{1}{2}}} \qquad (21)$$

where

$$r_1 = \frac{\omega}{\omega_1}$$

$$r_2 = \frac{\omega}{\omega_2}$$

$$\zeta_1 = \frac{\mu_1}{\omega_1}$$

$$\zeta_2 = \frac{\mu_2}{\omega_2}$$

$$\varepsilon = \tan^{-1} \frac{2[r_1\zeta_1(1 - r_2^2) + r_2\zeta_2(1 - r_1^2)]}{(1 - r_1^2)(1 - r_2^2) - 4r_1r_2\zeta_1\zeta_2}$$

$$= \tan^{-1} \frac{2r_1\zeta_1}{1 - r_1^2} + \tan^{-1} \frac{2r_2\zeta_2}{1 - r_2^2}$$

The amplitude ratio of the resultant motion is the product, and the phase lag the sum, of that from the separate mechanical and acoustic systems.

In practice the system will be used at forcing frequencies much lower than those of the acoustic and mechanical u.n.f.s. so that we may regard r_1 as small, and r_2 as negligibly small.

Thus, the time lag, $\tau = \frac{\varepsilon}{\omega} \mp \frac{2\zeta_1}{\omega_1}$

$$= \frac{8\eta}{\rho a^2} \cdot \frac{Q\ell}{\pi r^4} \qquad (22)$$

In this form it may be useful when designing installations, where, for reasons of accommodation, some changes in tube length must be accepted. The time lag will increase in proportion to the tube length providing ℓ is large compared with r.

(iv) Non-linear inputs at large incidences

For large angles the pressure is not a linear function of incidence (section 3) but proportional to sin 2θ. For harmonically programmed incidence ($\theta = \theta_o \sin \omega t$) the input function has the form $V = \frac{V_o}{2\theta_o} \sin(2\theta_o \sin \omega t)$ which, using the Sonine expansion, may be written as

$$V = V_o \cdot \frac{J_1(2\theta_o)}{\theta_o} \sin \omega t + \frac{V_o}{\theta_o} \sum_{n=1}^{\infty} J_{2n+1}(2\theta_o) \sin(2n+1)\omega t$$

where $J_n(2\theta_o)$ is a Bessel function of the first kind of integral order n.

The summed terms will produce distortion of the output, but this is estimated to be sufficiently small to be ignored even up to amplitudes of $\theta_o = 30^o$.

Summary of variables affecting acoustic response

For convenience the values of the relevant acoustic parameters, in terms of the pick-up and pressure tube dimensions and air properties, are summarised below. The mechanical mode parameters are not included since they are dependent on the stiffness of the diaphragm, a function of the edge constraints and the shape, and methods of calculating this quantity are already widely used in design offices.

ℓ = length of pressure tube from yawmeter head to pick-up

r = internal radius of pressure tube from yawmeter head to pick-up

Q = internal air volume of the pick-up

ρ = mean air density of air in the tube

η = mean dynamic viscosity of air in the tube

a = speed of sound in air in the tube

L_1 = acoustic inductance = $\frac{4}{3}\frac{\ell\rho}{\pi r^2}$

C_1 = acoustic capacitance = $\frac{Q}{\rho a^2}$

R_1 = acoustic resistance = $\frac{8\ell\eta}{\pi r^4}$

$\omega_1 = (L_1 C_1)^{-\frac{1}{2}} = a\left[\frac{3\pi r^2}{4\ell Q}\right]^{\frac{1}{2}}$

$\mu_1 = \frac{R_1}{2L_1} = \frac{3\eta}{\rho r^2}$

$\frac{\omega_1}{2\pi}$ = acoustic u.n.f. = $a\left[\frac{3r^2}{16\pi\ell Q}\right]^{\frac{1}{2}}$

$\frac{n_1}{2\pi}$ = acoustic damped n.f. = $\frac{\left[\omega_1^2 - \mu_1^2\right]^{\frac{1}{2}}}{2\pi} = \frac{1}{2\pi}\left[\frac{3a^2\pi r^2}{4\ell Q} - \frac{9\eta^2}{\rho^2 r^4}\right]^{\frac{1}{2}}$

ζ_1 = acoustic damping factor = $\frac{\mu_1}{\omega_1} = \frac{2\eta}{a\rho r^3}\left[\frac{3}{\pi}\ell Q\right]^{\frac{1}{2}}$

For a system forced harmonically at a frequency well below the acoustic u.n.f.

the time lag, τ, $\doteqdot \frac{2\zeta_1}{\omega_1} = \frac{8\eta}{\rho a^2} \cdot \frac{Q\ell}{\pi r^4}$.

4.2 Theoretical acoustic characteristics at supersonic speeds

The ultimate purpose of the response equation is to predict the behaviour of the instrument in free flight conditions, and to this end it is of interest to examine the theoretical relations between the frequency and damping in still air, in a supersonic wind tunnel and in free flight at ground level.

The mechanical u.n.f., being determined by the mass and stiffness of the spring system, should be the same in all conditions; a small change in damping factor might be expected arising from that part of the mechanical damping due to air resistance.

The acoustic u.n.f. is given theoretically by $a\sqrt{\frac{3r^2}{16\pi\ell Q}}$, and thus for any given instrument is proportional to the speed of sound in the air within the acoustic system, which again is determined entirely by the absolute temperature, T. In the present wind tunnel tests the yawmeter unit was not insulated thermodynamically from the tunnel wall so that its mean temperature was somewhere between room temperature and the

recovery temperature on the yawmeter head. The latter is of the order of 8° to 12°C below that of the room at the Mach Nos. of the tests. Since 'a' is proportional to $T^{\frac{1}{2}}$ there is a liklihood of a maximum reduction in the speed of sound of 1.4% and 2.1% at M = 1.4 and 1.9 respectively. From this it is apparent that the acoustic u.n.f. in supersonic wind tunnel conditions should differ only slightly, if at all, from that in still air. In flight at ground level the recovery temperature at supersonic speeds is considerably higher than the ambient air temperature ($T_F/T_S \div 1 + 0.18M^2$) so that the speed of sound within the instrument, and hence the acoustic frequency, will increase with Mach No. as $(1 + 0.18M^2)^{\frac{1}{2}}$.

The accustic damping factor, ζ_1, is theoretically $\frac{\eta}{a\rho}\frac{2}{r^3}\sqrt{\frac{3}{\pi}}\ell Q$

which, since η and a are both functions of T only and in the wind tunnel may be regarded as constant, means that ζ_1 is inversely proportional to the density, ρ, within the system. Further, since T is virtually the same in the wind tunnel as in still air, the density is inversely proportional to the mean pressure. This is the pressure at the inlet holes at zero incidence, and, from equation 4 is given approximately by $\frac{3p_o + p_s}{5}$. The wind tunnel tests were carried out at atmospheric stagnation pressure (i.e. the mean tube pressure during the pulse pressure tests in still air) which is $\left(1 + \frac{M^2}{5}\right)^{7/2}$ times the static pressure, p_s, in the tunnel when running at Mach No. M. Compared with the damping in still air therefore the damping factor in the wind tunnel increases as $5\left(1 + \frac{M^2}{5}\right)^{7/2} \div \left(\frac{3p_o}{p_s} + 1\right)$.

When, as in flight, there is a change of temperature within the system η/a is approximately proportional to $T^{0.3}$. Hence the damping factor in flight at ground level will be roughly $5(1 + 0.18M^2)^{1.3} \div \left(\frac{3p_o}{p_s} + 1\right)$ times that in still air. This function decreases with increase of M_1 and is shown in fig.11(a) together with the ratio for wind tunnel to still air conditions. The corresponding frequency ratios are shown in fig.11(b). Corresponding expressions can be developed for the damping factor at altitude by allowing for the effect of atmospheric temperature changes on η/a, and for the decrease in air density with height.

Summarising qualitatively, compared with the still air acoustic response the frequency in the wind tunnel should be unaltered but the damping increased, and in free flight at ground level the frequency should be increased and the damping reduced. The mechanical response should be virtually unaltered.

4.3 Measurement technique

Once the values of μ_1, μ_2, n_1 and n_2 have been determined the response of the instrument under any dynamic conditions may be obtained from equation 18 of 4.1 merely by inserting the function $\overline{V}$ and the initial conditions appropriate to the motion, and taking the inverse transform. The problem

is thus reduced to the determination of these parameters, which are functions of the separate acoustic and mechanical systems, under various conditions.

In the laboratory this was found to be most conveniently achieved by the application of an impulsive pressure, since, from equation 20 the response is in the form of two damped sine waves from which the frequencies and damping factors may be easily isolated. To obtain a close approximation to such an impulse a disc provided with a small hole was used to interrupt a compressed air jet directed into one of the yawmeter holes. The duration of the pulse was thus the time taken by the passage of the hole when the disc was in rotation.

The pressure was registered by the recorder as a spring displacement, and this was converted into a capacity change. This was automatically obtained with the capacity type pick-up, but for the bellows type recorder tiny capacity plates were fitted to the stylus arm. The changes in inertia and air damping so introduced were considered negligible. The capacity changes, which were of the order of 40 picrofarads maximum, were then transformed into voltage changes and applied to a Cossor type 1035 oscilloscope. A time base from a signal generator was included as a separate trace.

A typical response record produced by photographing the traces is shown in fig.16, the pressure pick-up in this case being the capacity type. The contributions from the separate systems are easily distinguished, the high frequency, lightly damped oscillation, due to the mechanical system, being modulated by the lower frequency acoustic oscillation. The equations of the separate envelopes, after allowing for the non-linearity of the trace displacement, gives the damping factors; the damped natural frequencies may be read off directly with reference to the time base, in this case 1000 c.p.s.

To examine the extent to which the parameters evaluated under still air laboratory conditions differed from those obtained when the instrument was operating in a supersonic airstream, experiments were made in the 9" supersonic wind tunnel (fig.12). The convenient pressure pulse method was no longer available, and two other programmes were accordingly considered. The first of these involved the application of a pressure "step" and the analysis of the ensuing transient response. The difficulty of obtaining a sufficiently short time of application of such a step was not overcome, however, although pneumatic and spring actuators were tried; and this method was abandoned in favour of a sinusoidal forcing programme.

In the earlier tests in which the bellows type pick-up was used the pressure registered was recorded as a displacement of a stylus over a celluloid strip. The incidence position was similarly recorded on a separate strip, and a time base common to both was superposed on each to enable the records to be aligned and the phase shift to be examined. Later as the development proceeded and the bellows pick-up was superceded by the capacity type transducer the incidence was recorded by a voltage pick-off from a potentiometer. In this way both incidence and pressure could be recorded simultaneously on a split beam oscilloscope and the phase shift measured more accurately. For these records the time base was included as an interruption of one or both traces.

4.4 Tests and results

As originally conceived the yawmeter was intended to be used in conjunction with the bellows type recorder shown in fig.13(a). The bulk of the latter would prevent it being positioned close to the missile nose, and it was envisaged that 20 inches of hypodermic tubing would be required to connect each yawmeter inlet hole to the recorder. This configuration

was first wind tunnel tested at M = 1.4 and 1.9, using tubing of 0.038 in. bore, and the celluloid records of the response to step and square wave pressure inputs are shown in Fig.15. It is apparent from these that the system was overdamped and the rate of application of the incidence too slow for it to be regarded as a true step from the point of view of analysis.

The relations of 4.1 show that the damping factor of the acoustic mode is theoretically $\frac{2\eta}{a\rho r^3} \cdot \sqrt{\frac{3}{\pi} \ell Q}$ so that it may be reduced by increasing the pipe radius and decreasing the length. The size of the pick-up precluded any decrease in length, but for the next wind tunnel tests the bore was increased to 0.053 in., and the instrument programmed harmonically to obviate the difficulties associated with step inputs. Extraction of the acoustic mode parameters then required the determination of the amplitude ratio of the output and input signal at particular forcing frequencies together with the phase shift (equation 21).

It was found in practice that at M = 1.4 the overall phase lag was large and was as much as 100° at 3.5 c.p.s. This is far greater than the acoustic theory would predict and is probably accounted for by a number of factors. Short lengths of rubber tubing were used to connect the yawmeter lines to the external recorder unit. Its flexibility enabled it to "breathe", and by so doing the acoustic capacity of the chamber volume would be increased. Also since the pressure inside was less than the room pressure it is possible that these tubes were compressed somewhat thereby increasing the acoustic resistance. This flexure has the effect of reducing the response frequency and increasing the damping factor although calculations suggest that the order of the changes is insufficient to account entirely for the large lag.

Another possible contributing factor is that the percentage volume change in the chamber under load is not small with this type of instrument. The acoustic capacity of the chamber can no longer be regarded as constant and equation 18 would require modifying accordingly.

One further possibility is that some of the damping may have been mechanical arising from the pressure on the stylus required to produce the record.

The main conclusion from the tests with this particular arrangement, viz. bellows type recorder with long pressure lines, was that the response is too slow for use in flight test work. The indications were that the response could be improved by

(i) reducing the length of tubing between the yawmeter head and the recorder,

(ii) reducing the volume of the pick-up chamber (and hence the acoustic capacity) to a minimum,

(iii) eliminating all flexible couplings,

(iv) the use of a pick-up sensitive to small changes of volume,

(v) eliminating sliding friction elements within the recorder.

All these factors pointed to the use of an existing capacity type pick-up suitable for measuring differential pressure. In this form the instrument is designed to have a full scale linear deflection of 0.002 inches,

corresponding to a maximum volume change of <0.5%, and giving for this range of movement a capacity change of approximately 30 microfarads. The yawmeter unit incorporating this pick-up is shown in fig.14; the length of tubing has been reduced from 20 inches to 5 inches, and the tubes are silver soldered to the pick-up. In this form the instrument is self-contained and suitable for fitting into a missile as a unit.

In fig.16 is shown the response of this version to a pressure pulse applied in still air conditions, and the superposition of the two modes (equation 20) is quite apparent. The high frequency (1050 c.p.s.) lightly damped (ζ = 0.05) oscillation is the mechanical mode (verified by vibrating the pick-up in the absence of the yawmeter head), and the low frequency (126 c.p.s.) is that of the acoustic system. The latter agrees well with that given theoretically (123 c.p.s.) but the damping factor of 0.22 is more than 50% higher than the theoretical value.

Fig.17 shows portions of the response records resulting from a disturbance in both still air and at M = 1.4. Two resonance frequencies are apparent, one of approximately 1000 c.p.s. corresponding to that of the mechanical mode and another of about 130 c.p.s. which is consistant with that of the acoustic mode as calculated and as measured in still air. Since these frequencies are evident in both traces it indicates that the frequency invariance in still air and in the wind tunnel is realised in practice.

The increase in the response frequencies with this pick-up compared with the bellows type meant that at forcing frequencies of the order of 2 to 3 c.p.s. the change in amplitude ratio of input and output signal would be too small to use in conjunction with the phase lag to evaluate the acoustic u.n.f. and damping factor. However, by taking the frequency under tunnel conditions as that determined outside the tunnel, only the damping factor remains unknown, and this can then be determined when the incidence is varied harmonically from a measurement of the phase shift above.

Sinusoidal forcing programmes were applied and as already described the incidence and pressure pick-off voltages applied to the oscilloscope. The beams, which were interrupted at 1000 c.p.s. to provide a time base were adjusted so that with the yawmeter at zero incidence to the stream both coincided with a thin blanking strip on the face of the oscilloscope tube. A phase shift at zero incidence during any subsequent programme was then shown by the time interval between traces of the separate beams crossing the blanked strip.

In fig.18 are shown parts of such a trace greatly enlarged, with high gain on the pressure pick-up beam (hence the cut-off except near the intersection). The yawmeter used in this case was an interim version (No.2) having the same pick-up and yawmeter head as the later, built-in version (No.6) but with a tube length of 20 inches instead of 5 inches. In the case shown the lag is seen to be 14 milliseconds. The theoretical relations of 4.1 predict a lag of 0.003 seconds so that the indications are that the damping obtained in practice with an oscillating instrument is roughly four times greater than the theoretical. Similar records were obtained with the shorter tube (built-in) version and the time lag was determined as 3 to 4 milliseconds. Both long and short tube instruments thus show this fourfold increase in damping, and incidentally provide a direct check of part of the predictions of equation 22, in which the time lag was shown to be proportional to the length of connecting tube.

To investigate this further the programming gear was modified to give forcing frequencies up to 45 c.p.s. and used to programme the built-in version over an incidence range of $\pm 5^{\circ}$. This necessitated operating the C.R.O. at high sensitivity for the pressure trace, and as a consequence of the light mechanical damping the pressure records at the highest speeds were modulated considerably by "mush" at the mechanical mode frequency (fig.19). Nevertheless it was possible to measure fairly reliably the phase lag between the incidence and pressure traces, and more approximately the amplitude ratios. The pick-offs were also applied to the oscilloscope plates to produce a closed Lissajou figure from which amplitude ratios and phase angles were again derived.

The phase angles at M = 1.4 and 1.9 using the built-in instrument were respectively 18.5° ($\pm 1.5^{\circ}$) and $23^{\circ}(\pm 1.5^{\circ})$ at a forcing frequency of 16.2 c.p.s., and $50^{\circ}(\pm 2^{\circ})$ and $56^{\circ}(\pm 5^{\circ})$ at 45 c.p.s. The equivalent damping factors regarding the acoustic u.n.f. as invariant and the contribution from the mechanical mode as negligibly small were $1.3(\pm 0.1)$ and $1.45(\pm 0.1)$ at M = 1.4, and $1.6(\pm 0.1)$ and $1.8(\pm 0.3)$ at M = 1.9. Compared with the theoretical values of 0.35 and 0.45 derived from that in still air and the relations of 4.2 the damping is once again greater by a factor of roughly $3\frac{1}{2}$ to 4. The equivalent time lag varies between 3 to 4 milliseconds. The amplitude ratios obtained from the derived damping factors and a u.n.f. of 126 c.p.s. are consistent with those measured within the limits of the indeterminancy produced by the mush.

4.5 Discrepancy between the response in still and supersonic air

Under still air conditions the frequencies and damping factors of the separate mechanical and acoustic systems have been measured, but the values so obtained, modified as required theoretically, are not consistent with the results of tests under supersonic conditions in which the overall time lag was measured.

A number of possible sources of this discrepancy require examination. The most likely explanation is that the acoustic damping is altered not only through a change in viscosity but also through a change in flow conditions within the tubes. The acoustic resistance, $\frac{8\ell\eta}{\pi r^4}$ is implicitly based on the assumption that the flow is laminar. It is in fact a form of Poiseuille's equation. A transition to turbulent flow could increase the resistance and hence the damping. There is only a small mass flow through the tubes, however, and the Reynolds No. is less than 100; this is so far below the accepted critical Reynolds No. ($\div 2000$) for transition that turbulent flow within the tubes when stationary is thought to be unlikely. It is possible however, that when the tubes are subject to a programme in incidence transition may be induced by the lateral acceleration to which they are subjected; in the present tests this acceleration ranged from 0.5 to 50g. No experimental data of pipe resistance under these conditions are known to the authors but it is felt that a transition to turbulent flow would increase the resistance at these low Reynolds Nos. as it does at higher Reynolds Nos. under normal transition conditions. It is also possible that separation and secondary flow within the tubes occurs during lateral acceleration. Under these turbulent and/or separated flow conditions the pressure drop will not be proportional to the volume flow so that the damping will in all probability be a function of the pressure amplitude.

The possibility that the centrifugal forces on the pick-up and air mass due to the rate of pitch are in some way responsible can, it is felt, be discounted. These give rise to a deflection of the diaphragm which

would be always in the same sense. The response curve would be distorted and the intersection of the pressure and incidence traces of fig.18 would be asymmetrical relative to the blanking strip instead of being symmetrically disposed on either side of it as recorded.

The alteration of flow direction due to the rate-of-pitch term can cause a phase lag of the input pressure. For example, the effective incidence in these conditions would be

$$\theta - \frac{R}{U}\dot{\theta}$$

where R = distance from the inlet holes to the centre of rotation

$$= \theta_o\left(\sin \omega t - \frac{R\omega}{U} \cos \omega t\right)$$

$$= \theta_o \sqrt{1 + \left(\frac{R\omega}{U}\right)^2} \sin (\omega t - \varepsilon) \qquad (23)$$

where $\varepsilon = \tan^{-1} \frac{R\omega}{U}$

For $R\omega$ small compared with the free stream velocity, U, $\varepsilon \doteq \frac{R\omega}{U}$

and the time lag $\left(= \frac{\varepsilon}{\omega}\right)$ is approximately constant as $\frac{R}{U}$, i.e. the time

taken for the external flow to traverse the distance between the pressure holes and the axis of rotation. In flight the latter would be the centre of gravity of the missile, and this distance might well be several feet. In these tests, however, it was only 3", so that the estimated time lag from this source is only of the order of 1.9×10^{-4} seconds at M = 1.4. The above treatment is doubtless an over simplification, and, as it is fashionable to regard crossflow behaviour around bodies of revolution as independent of axial and streamwise flow, wind tunnel tests were carried out over a range of subsonic speeds with the axis of the yawmeter normal to the flow direction. The results, given in fig.20, show that the differential pressure due to an independent crossflow is more nearly proportional to the square of the velocity in contrast with the implied linearity (for $\sin 2\theta \doteq 2\theta$) in the above. At velocities corresponding to $R\dot{\theta}$ in the dynamic tests the pressure change is negligibly small so that on neither basis is the explanation satisfactory.

This last possibility is a particular instance of lags arising from the fundamental difference between direct frequency/damping measurement and phase lag/amplitude measurement. These will obviously give the same results only if the circuit of fig.10 gives the whole picture. If, however, it is incomplete then the extra time lag may emanate from the omitted stage. For instance time lags in the instrumentation would add to those present in the acoustic-mechanical combination although in these tests the frequency of the electronic equipment was sufficiently high (2Mc/s) to render these negligible. There is, however, one possible omission, and for this we need to consider the assumptions on which equation 18 is based. It has been

assumed that the pressure attained at the inlet holes of the yawmeter is instantaneously that attained in the corresponding steady state incidence. If, however, there is any lag in the pressure build-up around the head, due to the external air behaving as a separate elastic system, then when the instrument is programmed harmonically this lag will, to a first approximation, be additive to that of the rest of the system. If this effect is significant then it could be important inasmuch as it sets an upper limit to the improvement which can be affected by development of the instrument itself.

The results are more consistent, however, with a factored increase in damping than with a more or less constant additional lag such as would be introduced by a finite build-up time. The indications are that the excessive damping under oscillatory conditions is real.

4.6 Further developments

If, as seems most likely, the increased phase shift is produced by premature transition or flow separation under lateral acceleration conditions, then it would seem that still further reduction in tube length is necessary to reduce the damping factor under those conditions to a desirable value (around 0.6). With the pressure pick-ups currently available this is not practicable, but it could be achieved by the development of a twin pressure cell sufficiently small to fit inside the hemispherical head. The small chamber volume and line air mass would increase the acoustic u.n.f., and the short length of pressure tubing would reduce the resistance and hence the damping factor. It is possible that such an arrangement would in fact have too little damping, but if this were so it could always be increased to any required value by including a restriction in the lines.

If means of measuring the ambient air pressure, other than by static pressure holes in the present instrument, are adopted then there is no purpose in retaining the cylindrical portion of the yawmeter. The hemisphere could be incorporated into the nose of the missile thereby reducing the tube length considerably. This arrangement would improve the dynamic response but, because of the change in shape aft of the hemisphere, it would require recalibration statically.

Mechanically, the damping of the capacity pick-up has been shown to be too light (0.05) and the instrument is being modified to include oil damping. This modification is also designed to reduce the effective internal volume of the pick-up to almost negligible proportions, thus greatly raising the acoustic natural frequency and lowering the damping of the acoustic system.

5 Conclusions

Static tests have been made up to incidences of 30° to provide calibration curves at Mach Nos. from 1.3 to 1.9. The instrument has been shown to resolve well when the body incidence is not in plane of a pair of holes, the maximum error at 30° being -4.2% at the particular Mach No. examined.

The sensitivity as a yawmeter is predicted closely by an expression somewhat similar in form to that given by the solution for incompressible flow around a sphere. In this form

$$\frac{\Delta p}{p_s} \div K_1\left(\frac{p_o}{p_s} - \tfrac{1}{2}\right) . \sin 2\theta$$

where K_1, from experiment, has values of 0.925 and 0.954 for hole dispositions, θ_o, of 45° and 53° respectively from the axis.

If the pressure, p_{pit}, from an axial pressure hole is measured as well, then

$$\theta \text{ in degrees} \doteq \frac{31 \frac{\Delta p}{p_s}}{\frac{p_{pit}}{p_s} - \frac{1}{2}} \quad \text{for } \theta_o = 45^\circ \text{ and}$$

$$\doteq \frac{30.1 \frac{\Delta p}{p_s}}{\frac{p_{pit}}{p_s} - \frac{1}{2}} \quad \text{for } \theta_o = 53^\circ$$

and the incidence is thus known without prior determination of the Mach No.

The pressure, p_{pit}, decreases with incidence closely as $\left(\frac{p_{pit}}{p_s} - \frac{1}{2}\right) \div \left(\frac{p_o}{p_s} - \frac{1}{2}\right) \cos^{3/2}\theta$. Again $\frac{p_o}{p_s}$, and hence Mach No. may be derived without prior knowledge of the incidence from

$$\frac{p_o}{p_s} \doteq \frac{p_{pit}}{p_s} + \frac{0.22 \left(\frac{\Delta p}{p_s}\right)^2}{\left(\frac{p_{pit}}{p_s} - \frac{1}{2}\right)}$$

Roll angle is given to within 2° up to 30° incidence at the combined plane by $\tan^{-1}\left(\frac{\Delta p_2}{\Delta p_1}\right)$.

The pressure on the cylindrical body at incidence can differ so widely from that of the free stream that it is considered unlikely that this instrument can conveniently be used to measure the static pressure. It is usually possible, however, to obtain this under trials conditions from trajectory and meteorological data.

Providing this information is available the Mach No., incidence and roll angle may be derived, either from the above relations or from calibration charts, in terms of the ratios of the pitot and differential pressures to the free stream static pressure.

Dynamically the bellows type recorder has been found unsuitable for use with this instrument due to the low acoustic natural frequency and the length of pressure tubing required. The response was greatly improved by using a small capacity type pick-up with shorter pressure tubes; the mechanical and acoustic u.n.f.'s were found to be 1050 and 126 c.p.s. respectively. Further improvement is hoped for as a result of impending modifications to the pick-up. These include a greater reduction of the internal volume and the provision of a variable degree of damping.

There is evidence that when the instrument is subjected to a lateral acceleration such as it would encounter in flight the damping factor of the response is much higher than that predicted from theory and from measurements in the absence of any lateral acceleration. Possible causes of this were examined and it is thought most likely that it derives from increased acoustic resistance in the pressure lines as a result of transition and, possibly, flow separation in the tubing when accelerated laterally.

REFERENCES

No.	Author	Title, etc.
1	Olson, H.F.	"Elements of acoustical engineering". D. Van Nostrand Co. Inc. 1940.
2	Hutton, P.G.	Static response of a hemispherical-headed yawmeter at high subsonic and transonic speeds. C.P. No.401. August, 1957.

APPENDIX I

Effect of inaccurate pressure hole location

In the manufacture of these instruments, even when the pressure holes are jig-bored, there will inevitably be small location errors, which, if allowance is not made for them, can introduce errors into the incidence and roll angle measurements. Providing the manufacturing errors are known it is possible to correct the indicated quantities accordingly.

There are two results of inaccurate location. The joins of each pair of holes may not be mutually perpendicular, and their intersection, hereafter referred to as the virtual centre, may not be on the yawmeter axis. The angular errors are assumed to be less than half a degree, so that the errors from the first source, being of second order, may be neglected. The second introduces a small misalignment error, θ_E, as a a roll angle, ϕ_E, (not necessarily small) relative to a datum fixed in instrument (fig.21). Denoting the angles between the yawmeter axis and the radii through the separate holes by θ_{01}, θ_{02} etc, then, to first order, we have that the virtual centre is removed from the axis a distance $R_s\left[(\theta_{01} - \theta_{03})^2 + (\theta_{04} - \theta_{02})^2\right]^{\frac{1}{2}} \div 2\sqrt{2}$, where R_s is the radius of the sphere, the holes are numbered consecutively clockwise and the nominal value of θ_o is 45. The angle, θ_E, subtended at the centre of the sphere is thus $\frac{1}{2}\left[(\theta_{01} - \theta_{03})^2 + (\theta_{04} - \theta_{03})^2\right]^{\frac{1}{2}}$. The misalignment roll angle, ϕ_E, referred to hole 1, is given by

$$\phi_E = \tan^{-1} \frac{\theta_{02} - \theta_{04}}{\theta_{01} - \theta_{03}} \qquad (24)$$

If we denote the indicated quantities by suffix I then it is readily seen from fig.21 that

$$\left.\begin{aligned} \sin\theta \sin\phi &= \sin\theta_I \sin\phi_I + \theta_E \sin\phi_E \\ \sin\theta \cos\phi &= \sin\theta_I \cos\phi_I + \theta_E \cos\phi_E \end{aligned}\right\} \qquad (25)$$

from which

$$\tan\phi = \frac{\sin\theta_I \sin\phi_I + \theta_E \sin\phi_E}{\sin\theta_I \cos\phi_I + \theta_E \cos\phi_E} \qquad (26)$$

$$\sin^2\theta = \sin^2\theta_I + \theta_E^2 + 2\theta_E \sin\theta_I \cos(\phi_E - \phi_I) \qquad (27)$$

In practice θ_{01}, etc. will be known from the inspection report for each instrument so that θ_E and ϕ_E can be determined and the indicated values corrected from equations 26 and 27.

APPENDIX II

Condition that $2\bar{Z}_1\bar{Z}_3 \ll \bar{Z}_2(\bar{Z}_1 + \bar{Z}_3)$

In equation 18 the denominator of equation 17, $\bar{Z}_1\bar{Z}_2 + \bar{Z}_2\bar{Z}_3 + 2\bar{Z}_1\bar{Z}_3$, has been replaced by $Z_1Z_2 + Z_2Z_3$ for convenience in solving the response equation,

where
$$\bar{Z}_1 = L_1S + R_1$$
$$\bar{Z}_2 = L_2S + R_2 + \frac{1}{C_2S}$$
$$\bar{Z}_3 = \frac{1}{C_1S}$$

If $2\bar{Z}_1\bar{Z}_3 \ll Z_2(Z_1 + Z_3)$, then, by equating coefficients of powers of S,

$$2L_1 \ll L_2 + \frac{L_1C_1}{C_2} + R_1R_2C_1 \tag{28}$$

and
$$2R_1 \ll R_2 + \frac{R_1C_1}{C_2} \tag{29}$$

Rewriting and substituting $\zeta = \frac{R}{2L\omega} = \frac{RC\omega}{2}$ and $\omega = \frac{1}{LC}$

these conditions become,

$$\frac{L_1}{L_2} \ll \tfrac{1}{2}\left[1 + \left(\frac{\omega_2}{\omega_1}\right)^2 + 4\zeta_1\zeta_2\frac{\omega_2}{\omega_1}\right] \tag{30}$$

and
$$\frac{L_1}{L_2} \ll \tfrac{1}{2}\frac{\omega_2}{\omega_1}\cdot\frac{\zeta_2}{\zeta_1} + \tfrac{1}{2}\left(\frac{\omega_2}{\omega_1}\right)^2 \tag{31}$$

Since $\zeta_1\zeta_2$, ω_2 and ω_1 are essentially positive, we may write, more restrictedly,

$$\frac{L_1}{L_2} \ll \tfrac{1}{2}\left(\frac{\omega_2}{\omega_1}\right)^2 \tag{32}$$

Now $L_1 = \frac{4\ell\rho}{3\pi r^2} = \frac{4}{3}\cdot\frac{m_1}{A_1^2}$

$L_2 = \frac{m_2}{A_2^2}$

where m_1 = mass of line air
A_1 = line cross-section area
m_2 = mass of pick-up moving parts
A_2 = chamber cross-section area.

Thus the requirement is satisfied providing

$$\frac{L_1}{L_2} \equiv \frac{4}{3}\left(\frac{m_1}{m_2}\right)\left(\frac{A_2}{A_1}\right)^2 \ll \frac{1}{2}\left(\frac{\omega_2}{\omega_1}\right)^2 \qquad (33)$$

For the built-in capacity pick-up

$m_1 = 5.38 \times 10^{-7}$ lbs

$m_2 = 1.78 \times 10^{-2}$ lbs

$A_1 = 2.21 \times 10^{-3}$ ins^2

$A_2 = 0.407$ ins^2

$\omega_2 = 1050$ c.p.s.

$\omega_1 = 123$ c.p.s.

$$\therefore \frac{L_1}{L_2} = 3.7\% \text{ of } \frac{1}{2}\left(\frac{\omega_2}{\omega_1}\right)^2$$

APPENDIX III

An example of the data extraction methods of para.3.5

The following pressure ratios are applicable to $\theta = 25^{\circ}$, $M = 1.4$ and $\phi = 52^{\circ}$, using the No.2 yawmeter for which $\theta_o \doteq 45$:-

$$\frac{\Delta p_1}{p_s} = 1.09 \quad ; \quad \frac{\Delta p_2}{p_s} = 1.46 \quad ; \quad \frac{p_{pit}}{p_s} = 2.70.$$

Starting with these pressure ratios let us derive M, θ and ϕ as detailed in para.3.5.

First approximation

Firstly obtain the approximate pressure ratio in the combined plane from equation 7

$$\text{viz.} \quad \frac{\Delta p}{p_s} \doteq \left[\left(\frac{\Delta p_1}{p_s}\right)^2 + \left(\frac{\Delta p_2}{p_s}\right)^2\right]^{\frac{1}{2}} = 1.82$$

From fig.9(b) using this value, and $\frac{p_{pit}}{p_s} = 2.7$ we have for first approximations

$$\underline{\theta = 25.8}$$
$$\underline{M = 1.40_3}$$

Second approximation

Method 1 For $M = 1.40_3$, $\frac{\Delta p_1}{p_s} = 1.09$ and $\frac{\Delta p_2}{p_s} = 1.46$, we have from fig.9(b),

$$\underline{\alpha_1 = 14.3^{\circ}}$$
$$\underline{\alpha_2 = 19.6^{\circ}}$$

From equation 6 the second approximation to θ is:-

$$\sin\theta = \left[\sin^2\alpha_1 + \sin^2\alpha_2\right]^{\frac{1}{2}}, \quad \text{giving} \quad \theta = 24.6^{\circ}$$

From equation 6

$$\tan\phi = \frac{\sin\alpha_2}{\sin\alpha_1} \quad \text{giving} \quad \underline{\phi = 53.6^{\circ}}$$

Method 2 Alternatively we may use equation 8 to correct for $\frac{\Delta p}{p_s}$ taking

$\phi \div \tan^{-1}\left(\frac{\Delta p_2}{p_s} \div \frac{\Delta p_1}{p_s}\right) = 53.3^\circ$, and the first approximation to $\theta(=25.8^\circ)$.

Thus

$$\text{error} \div \sec\theta\left[1 - \sin^2\theta(\cos^4\phi + \sin^4\phi)\right]^{\frac{1}{2}} - 1$$

$$= 0.05$$

Hence corrected $\frac{\Delta p}{p_s} = 1.77$, which in conjunction with $\frac{p_{pit}}{p_s} = 2.70$

gives from fig.9(b)

$$\underline{\theta = 25.1^\circ}$$
$$\underline{M = 1.39_8}$$

Approximation from functional form

The approximation of equation 9 gives for θ, using

$$\frac{\Delta p}{p_s} \div \left[\left(\frac{\Delta p_1}{p_s}\right)^2 + \left(\frac{\Delta p_2}{p_s}\right)^2\right]^{\frac{1}{2}}$$

$$\theta \div \frac{31\,\frac{\Delta p}{p_s}}{\frac{p_{pit}}{p_s} - \frac{1}{2}} \quad \text{i.e.} \quad \underline{\theta = 25.6}$$

Also $$\frac{p_o}{p_s} = \frac{p_{pit}}{p_s} + \frac{0.22\left(\frac{\Delta p}{p_s}\right)^2}{\frac{p_{pit}}{p_s} - \frac{1}{2}}$$ from equation 12

$$= 3.03$$

$\therefore$ From fig.8, or tables, $\underline{M = 1.400}$

WT.2078.C.P.414.K3 - Printed in Great Britain

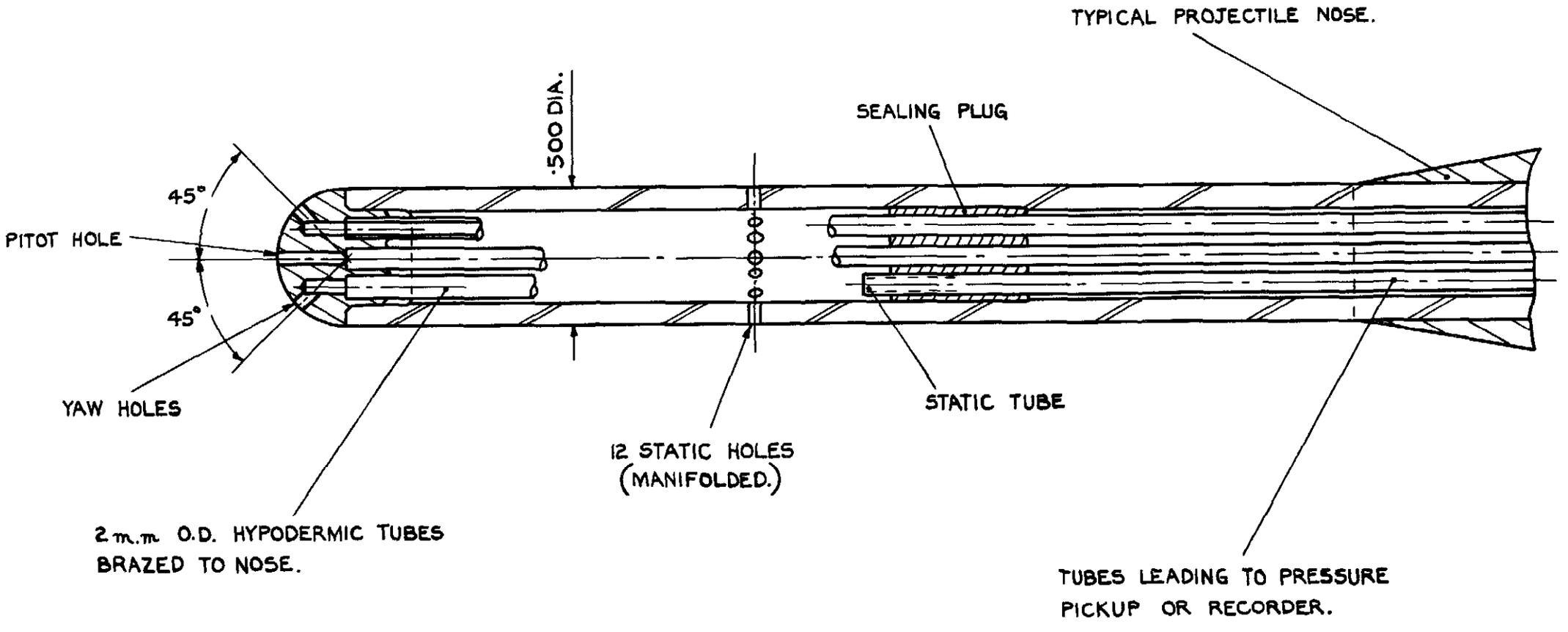

FIG. 1. YAWMETER HEAD ASSEMBLY.

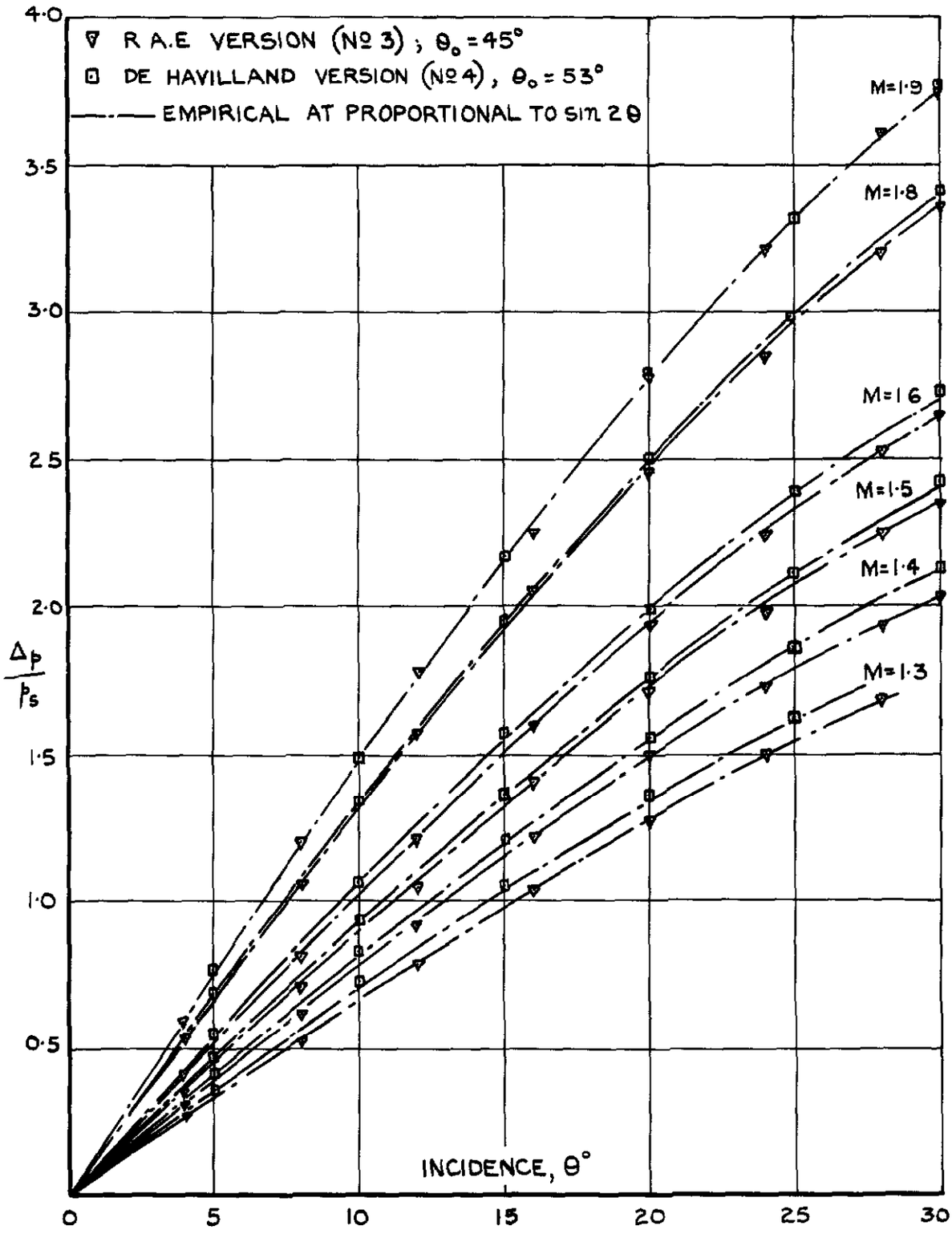

FIG.2. CALIBRATION CURVES OF DIFFERENTIAL PRESSURE VERSUS INCIDENCE.

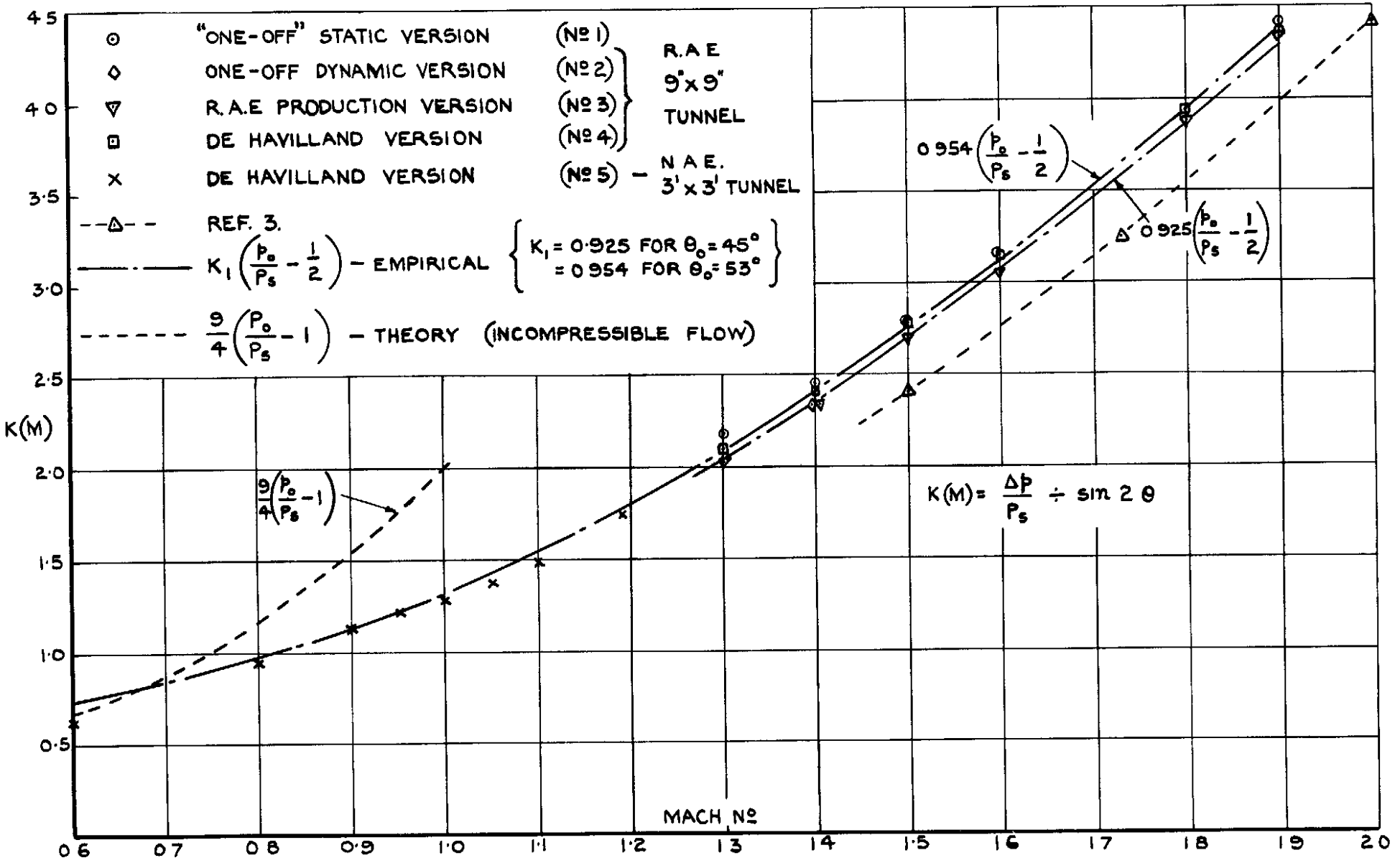

FIG.3. VARIATION OF SENSITIVITY WITH MACH No.

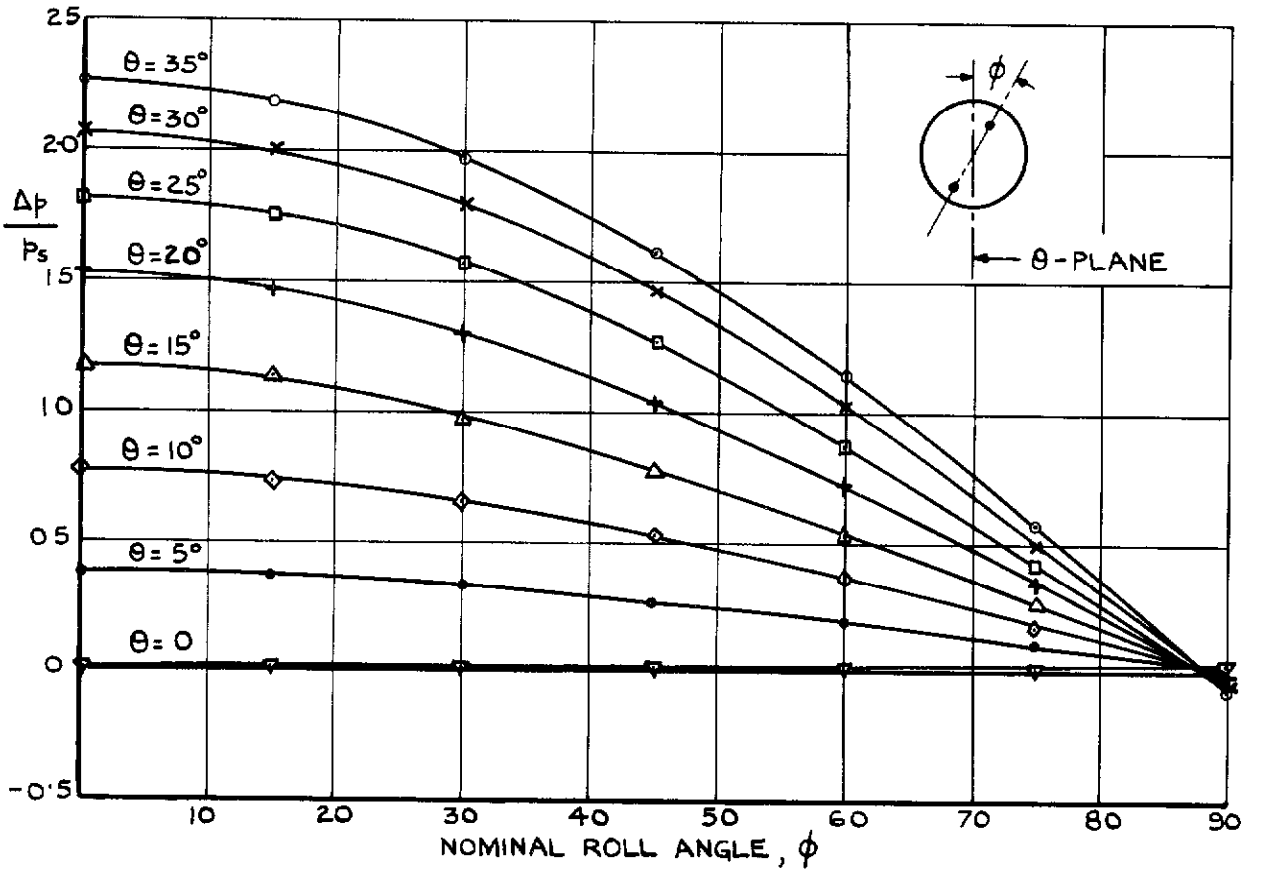

FIG.4. VARIATION OF DIFFERENTIAL PRESSURE WITH ROLL ANGLE.

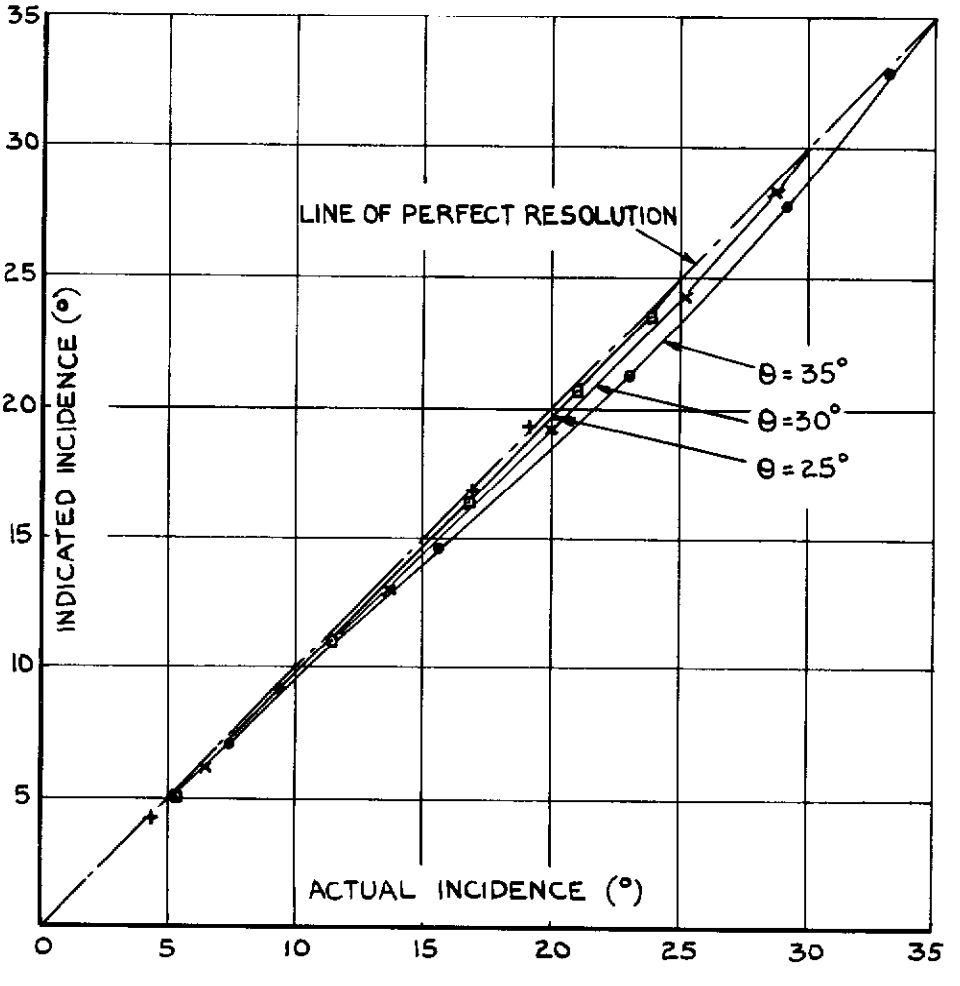

FIG.5. RESOLUTION IN PITCH AND YAW.

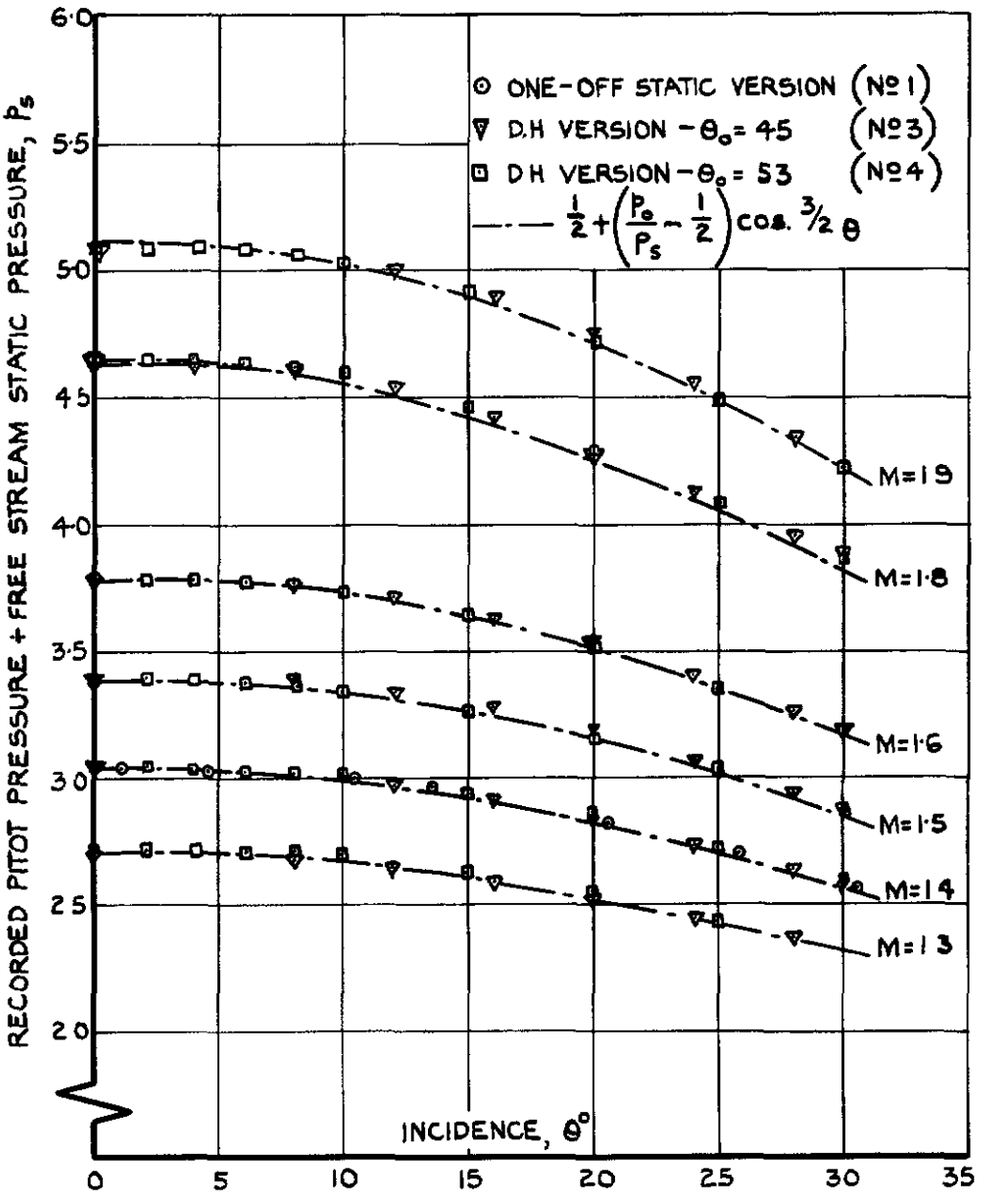

FIG.6. VARIATION OF PITOT PRESSURE WITH INCIDENCE.

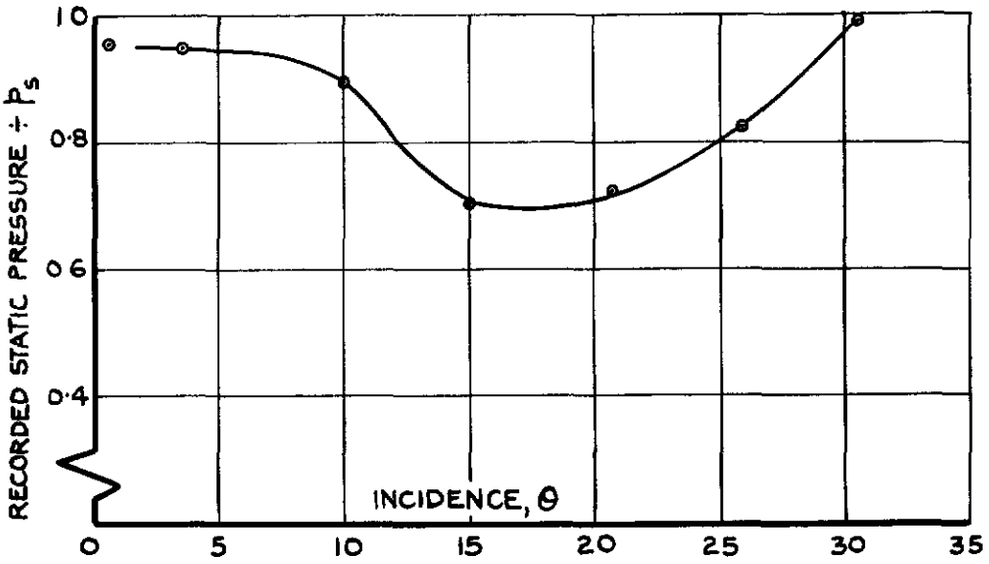

FIG.7. RECORDED STATIC PRESSURE VARIATION WITH INCIDENCE.

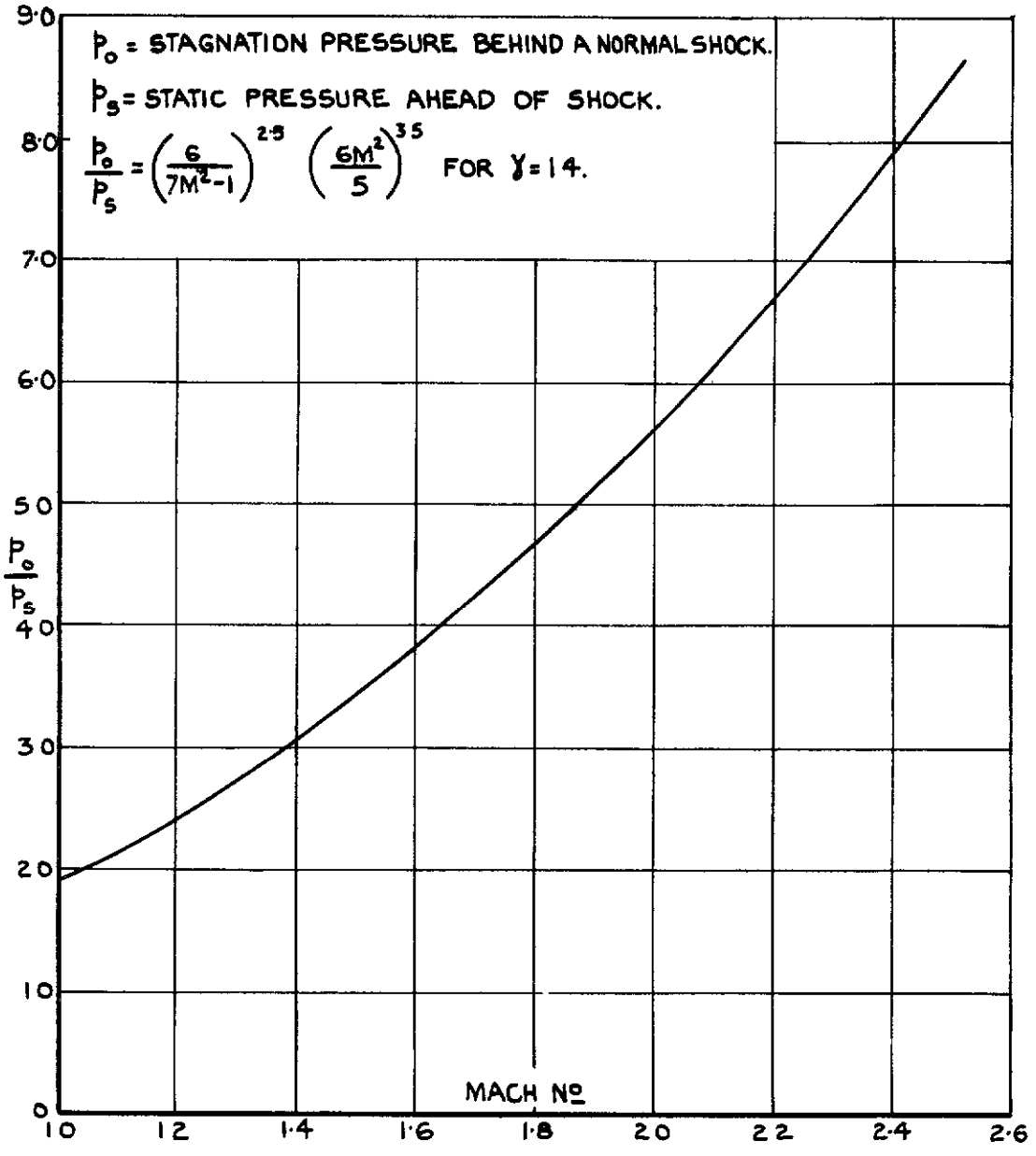

FIG.8. RELATION BETWEEN MACH Nº. AND P_o/P_s.

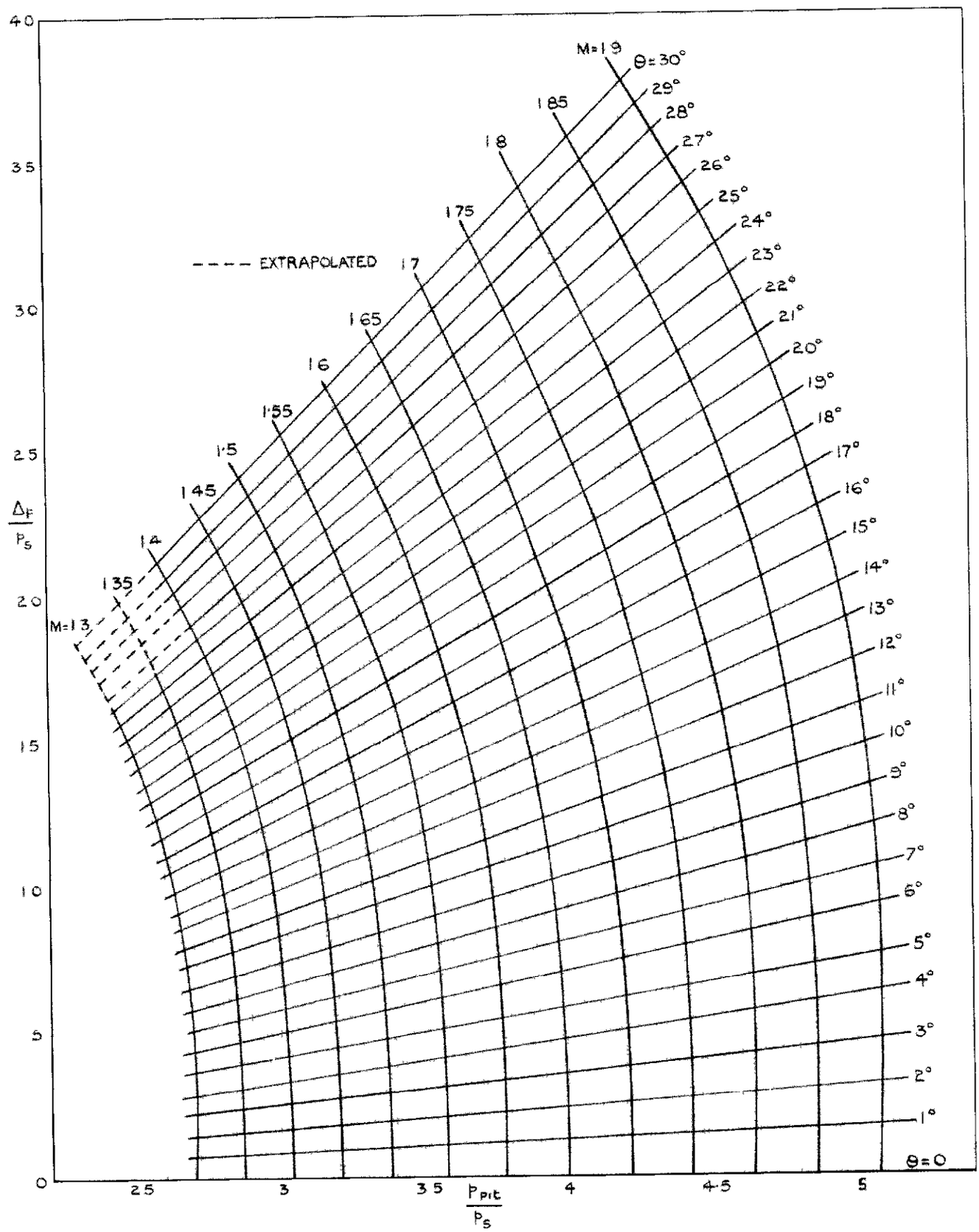

FIG.9(a). CHART FOR THE DETERMINATION OF θ AND M IN TERMS OF THE PITOT PRESSURE AND DIFFERENTIAL PRESSURE IN THE COMBINED PLANE ($\theta_0 = 53°$).

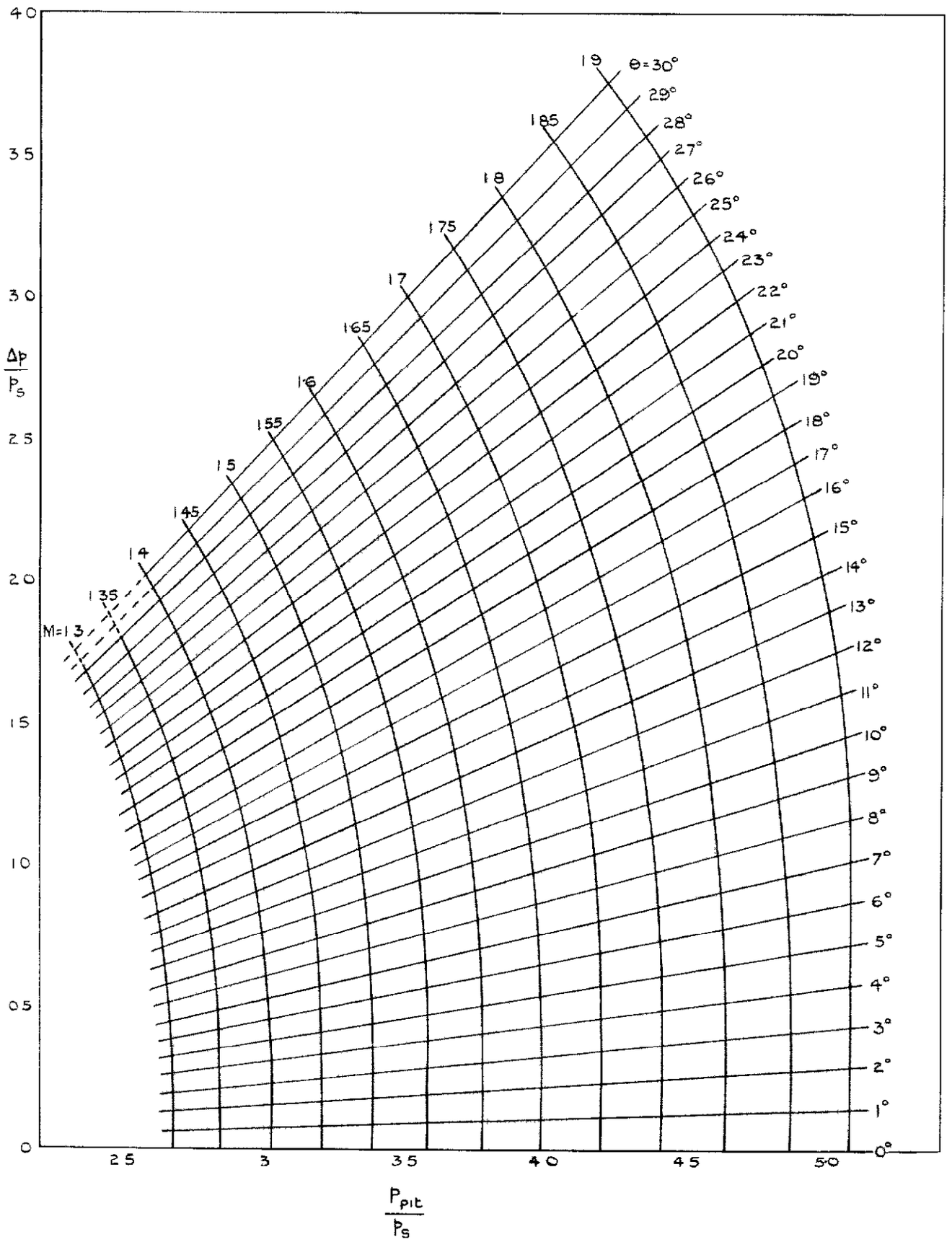

FIG 9 (b) $\theta_o = 45°$

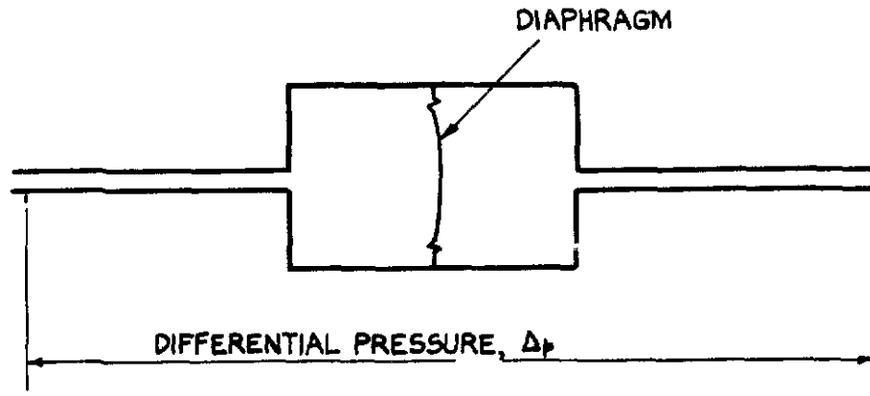

(a) ACOUSTIC - MECHANICAL SYSTEM.

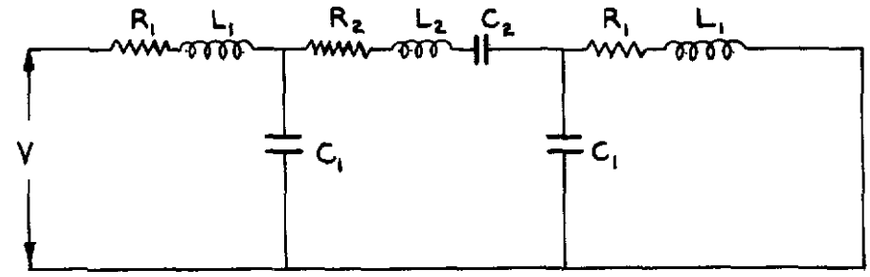

(b) ELECTRICAL ANALOGUE OF (a)

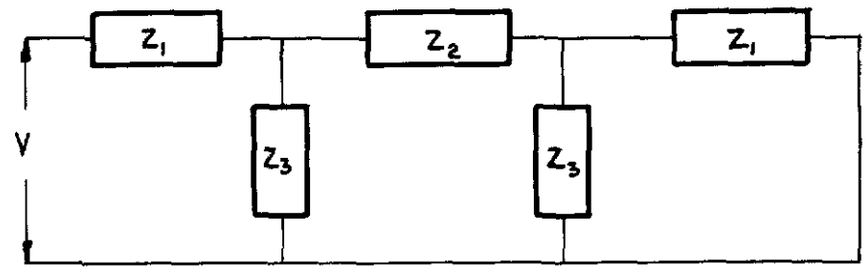

(c) GENERALISED FORM OF (b)

FIG.10(a-c). ELECTRICAL ANALOGUE OF YAWMETER AND PICK-UP SYSTEM.

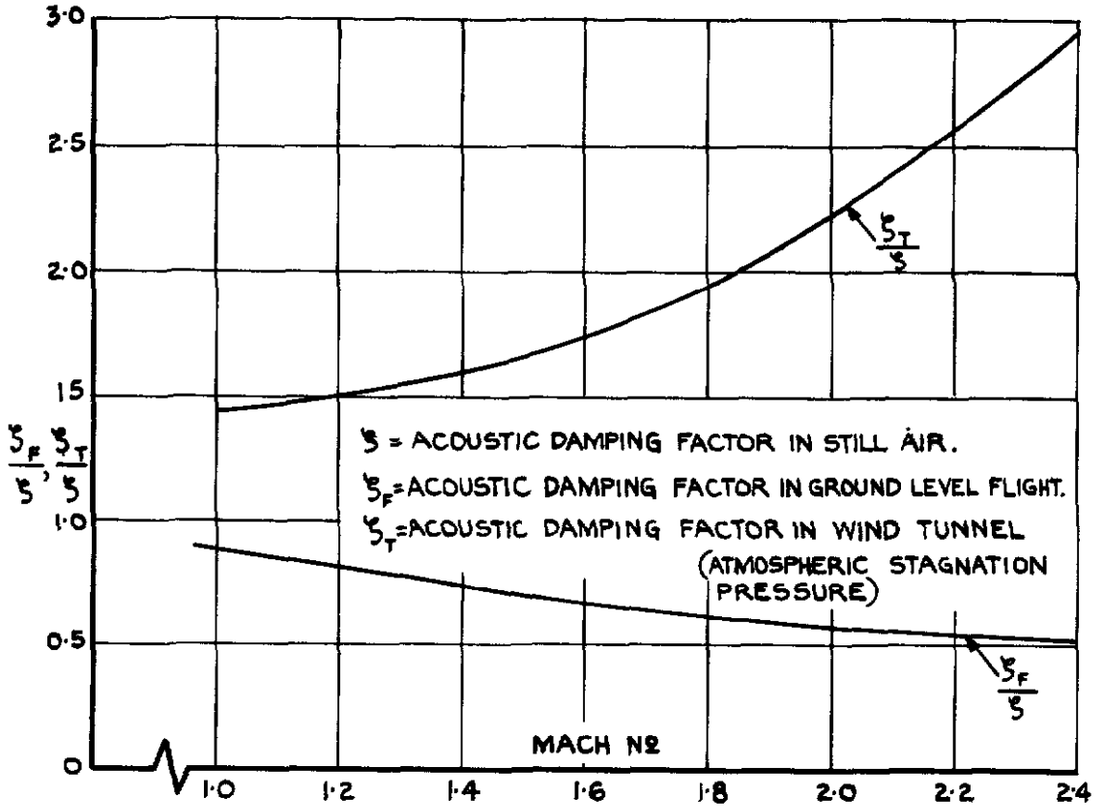

(a) DAMPING FACTOR

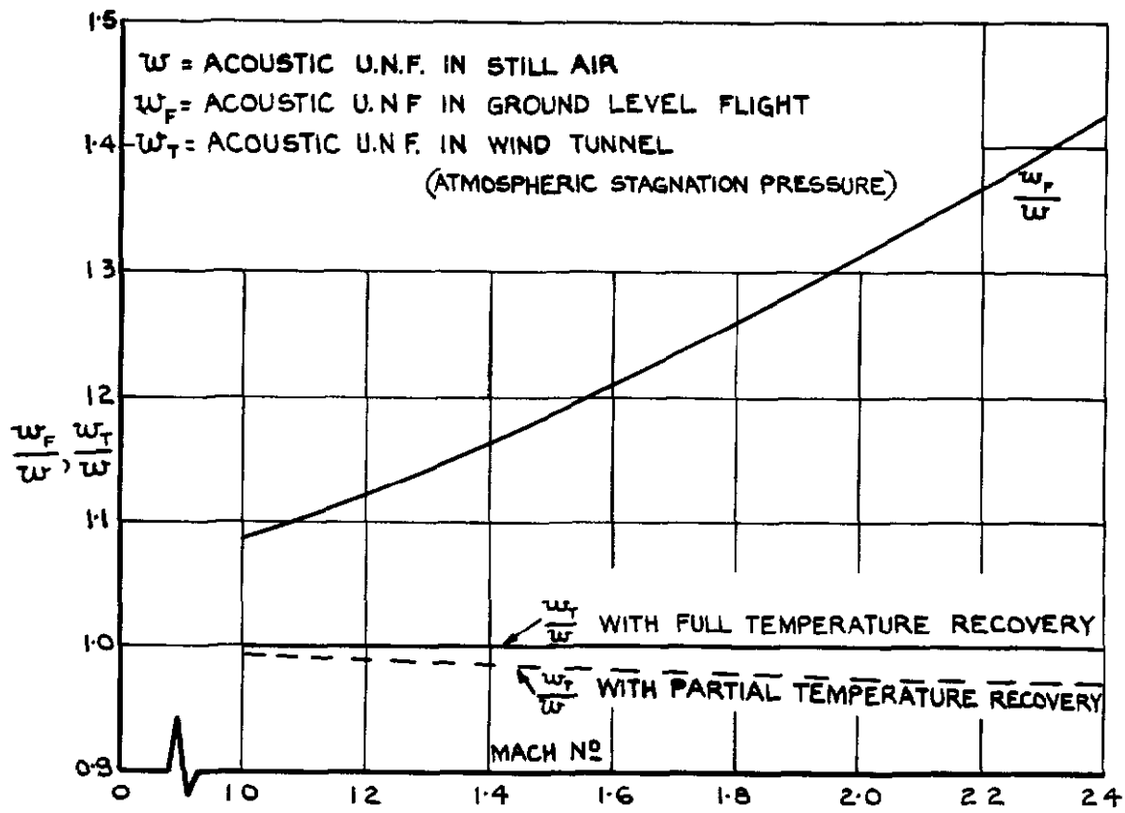

(b) ACOUSTIC U.N.F.

FIG.11(a & b). RELATIONS BETWEEN ACOUSTIC DAMPING AND U.N.F. IN FLIGHT AND WIND TUNNEL AND THAT IN STILL AIR.

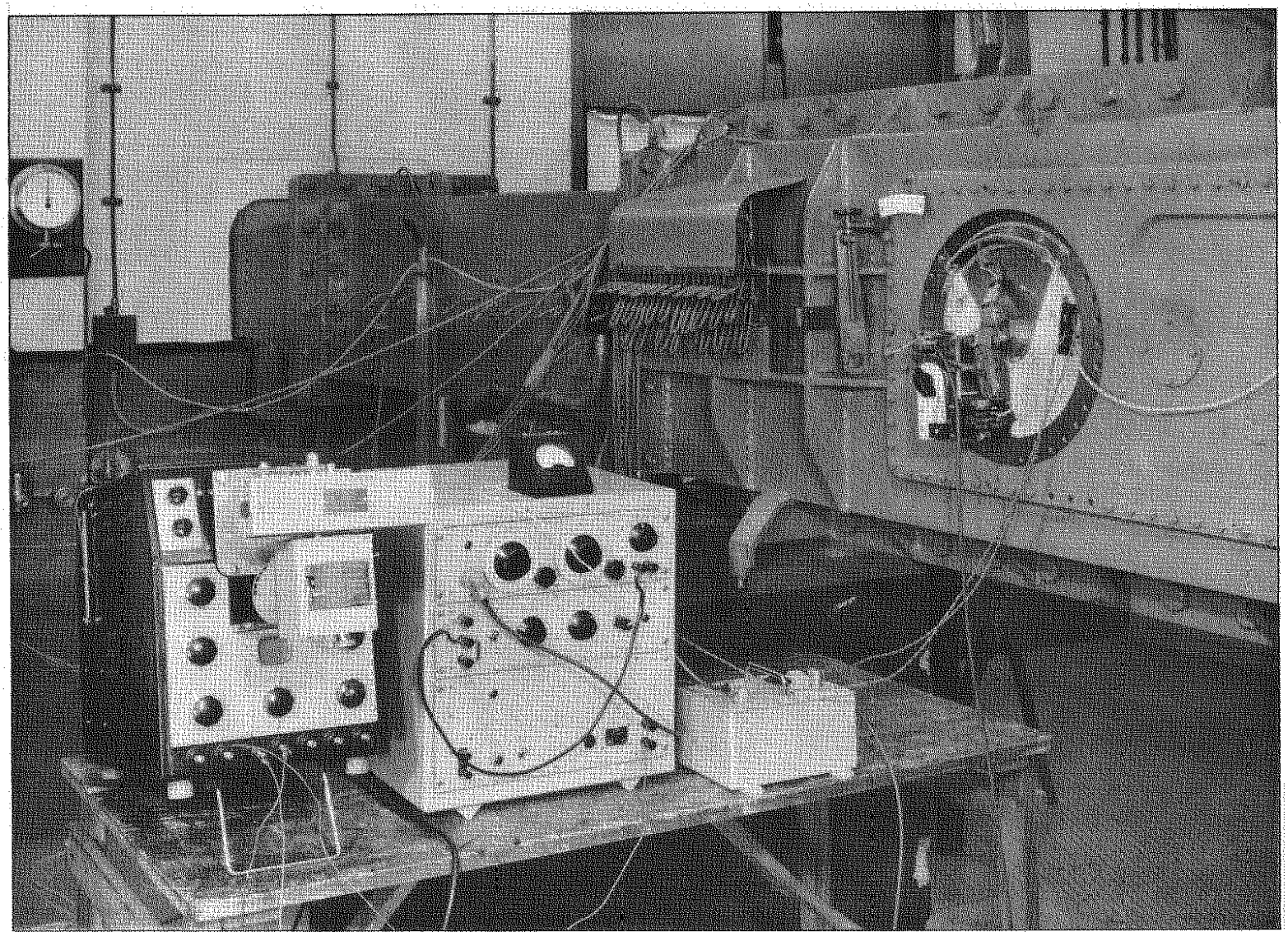

FIG.12. DYNAMIC TEST EQUIPMENT

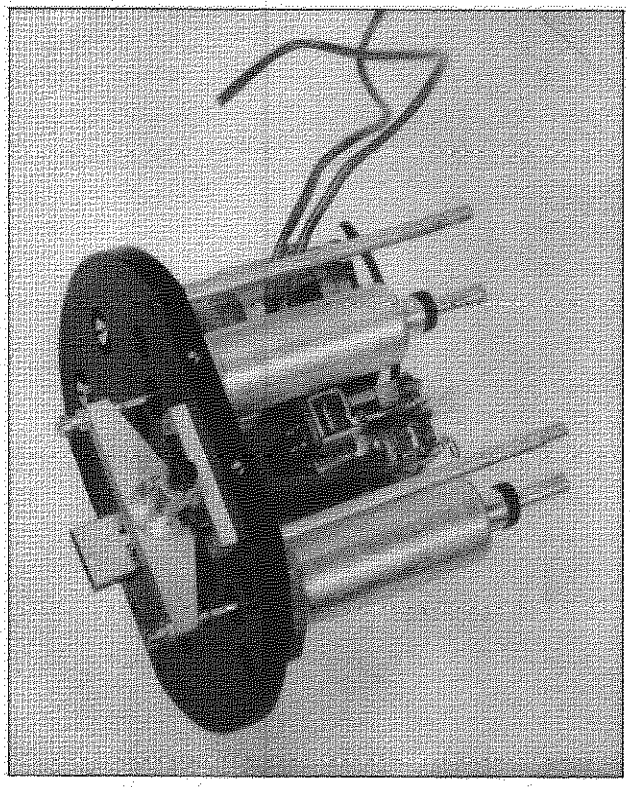

a. BELLOWS TYPE

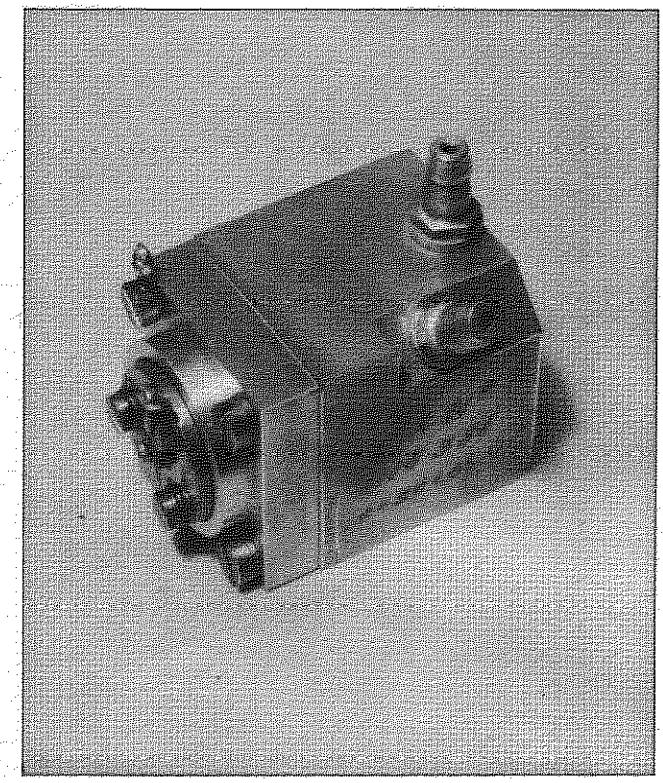

b. CAPACITY TYPE

FIG.13. PRESSURE PICK-UP

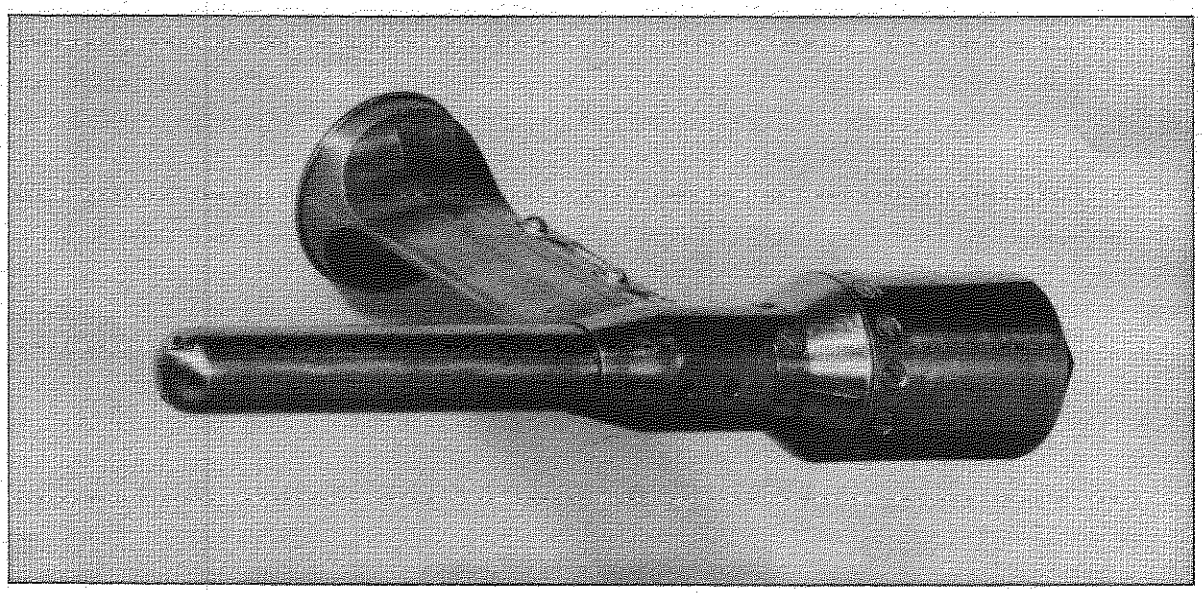

FIG.14. YAWMETER WITH BUILT-IN CAPACITY TYPE PICK-UP

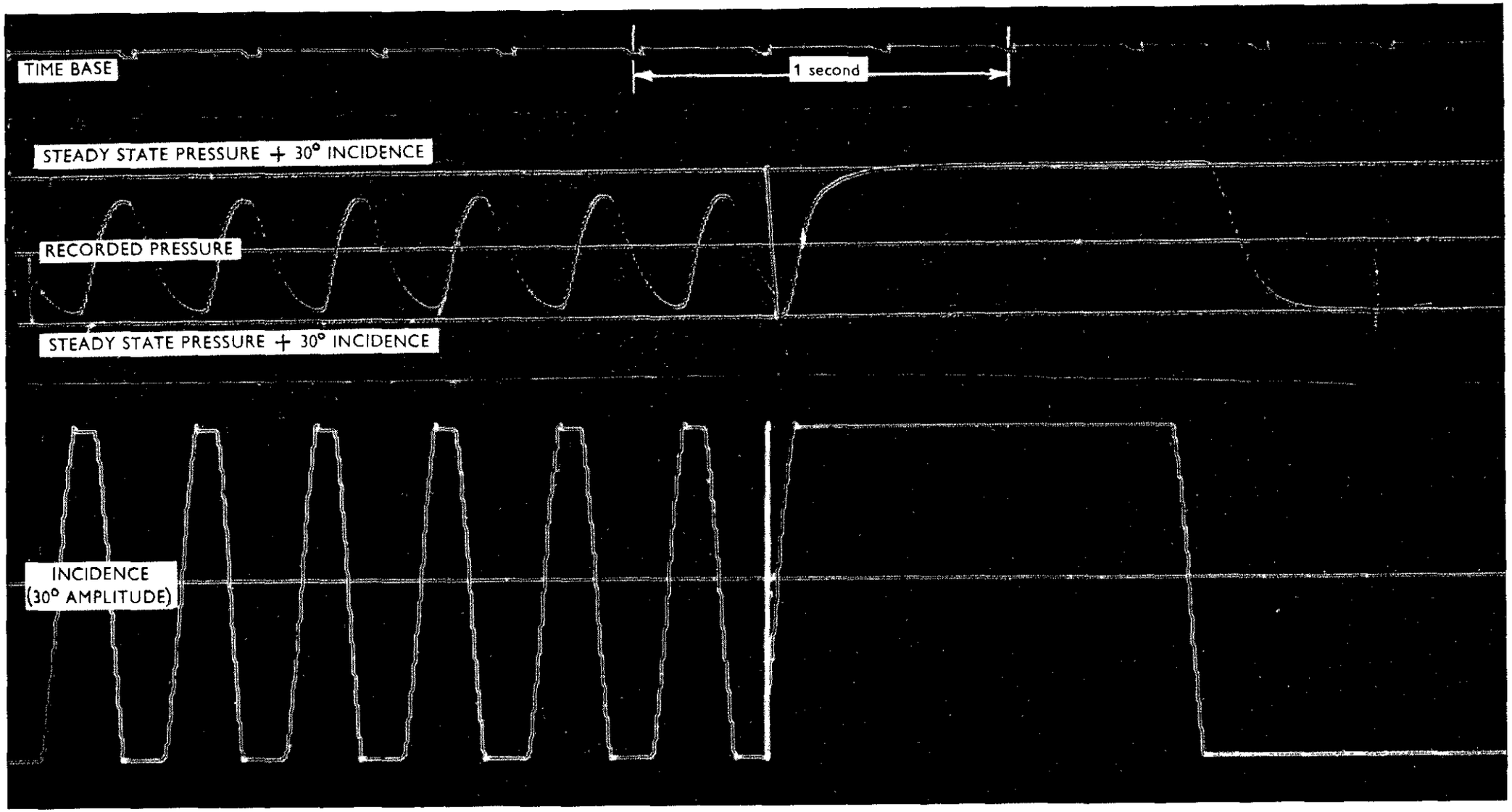

FIG 15. PRESSURE RESPONSE OF YAWMETER WITH BELLOWS PRESSURE RECORDER

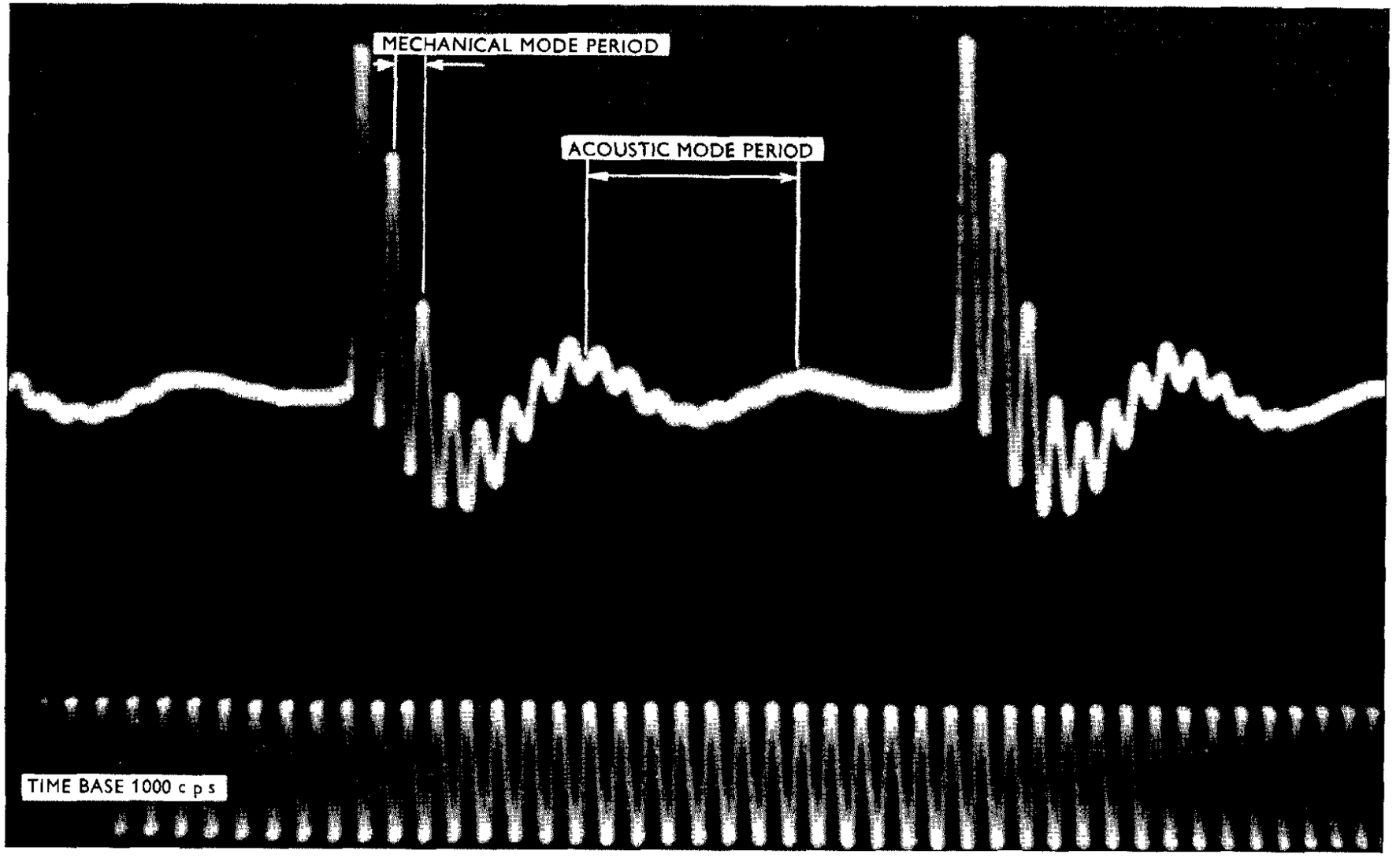

FIG 16 PRESSURE RESPONSE OF YAWMETER WITH BUILT-IN CAPACITY PICK-UP TO AN IMPULSE IN STILL AIR

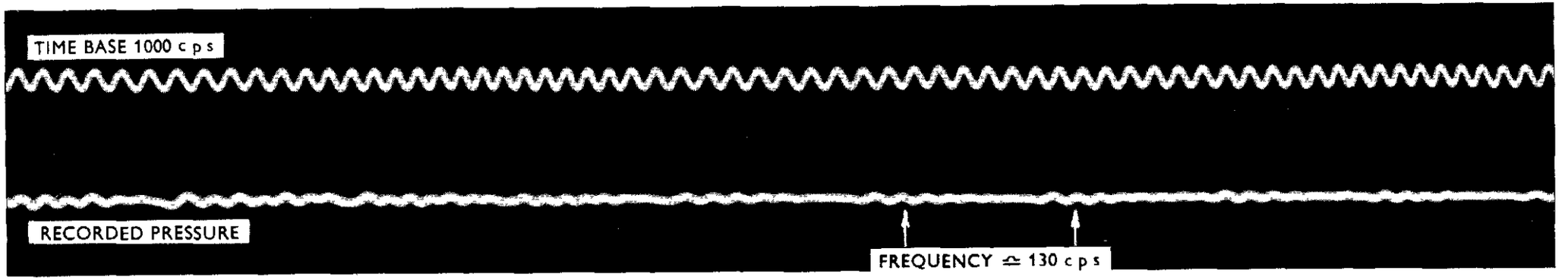

a STILL AIR

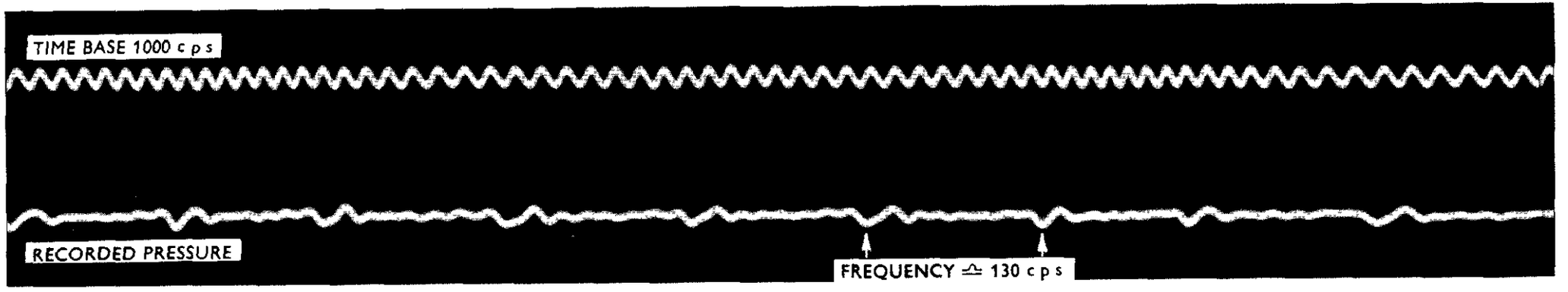

b M = 1 4 IN WIND TUNNEL

FIG 17 RESPONSE OF BUILT-IN VERSION TO MECHANICAL VIBRATION

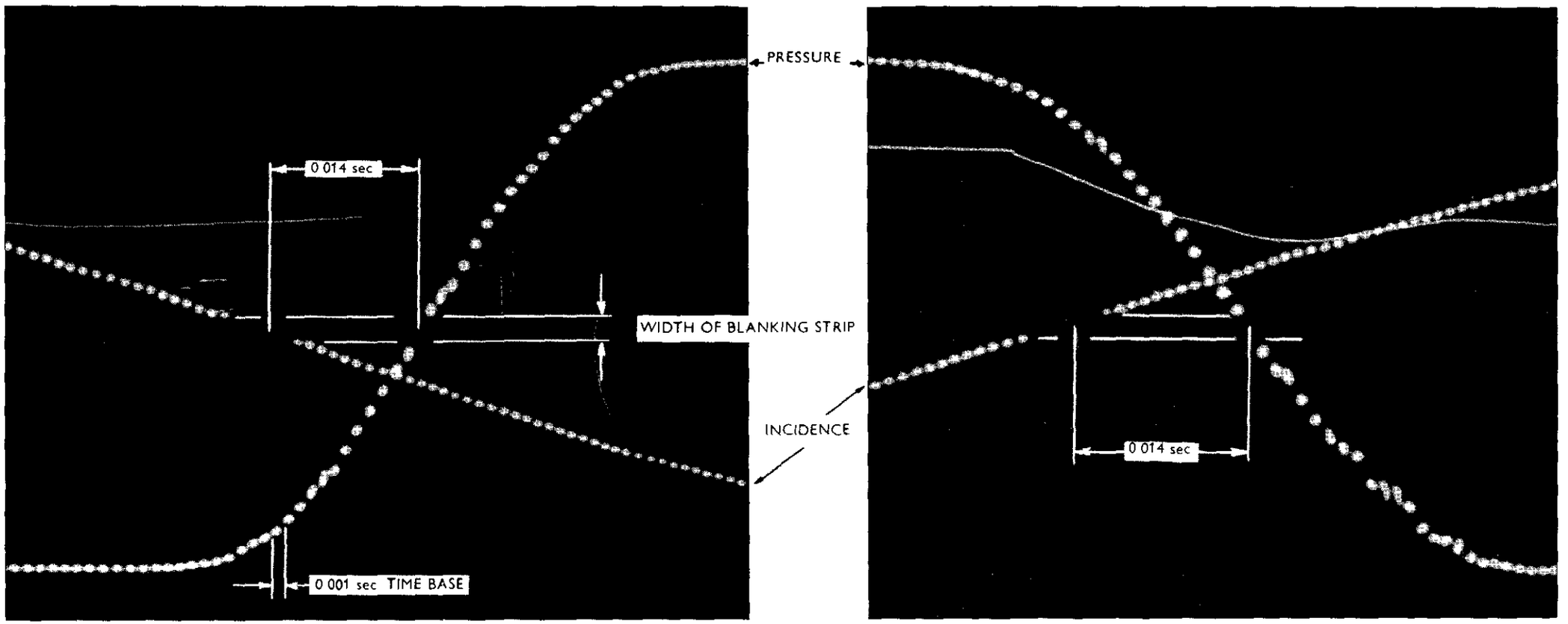

FIG 18 TIME LAG OF INTERIM (LONG TUBE) VERSION PROGRAMMED 15° AT 3 c p s (M = 1 9)

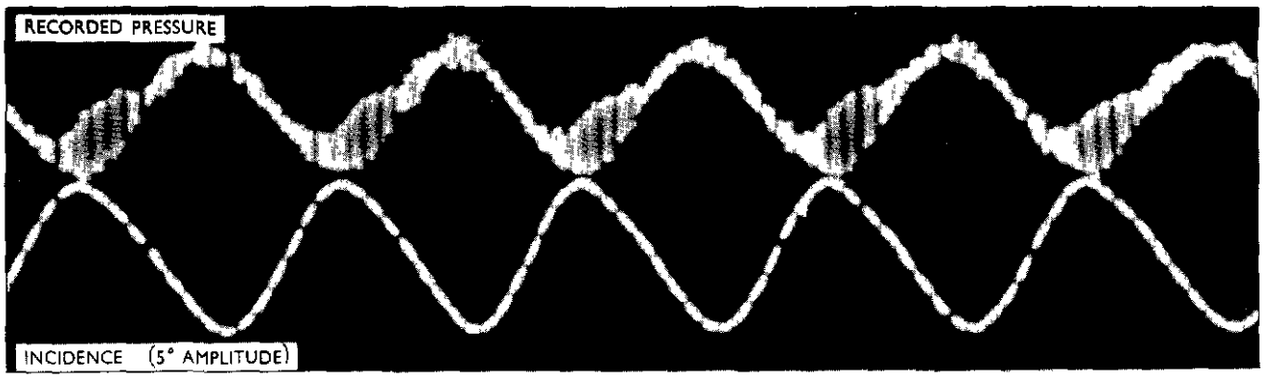

FORCING FREQUENCY = 16·2 c p s TIME BASE 250 c p s M = 1·4

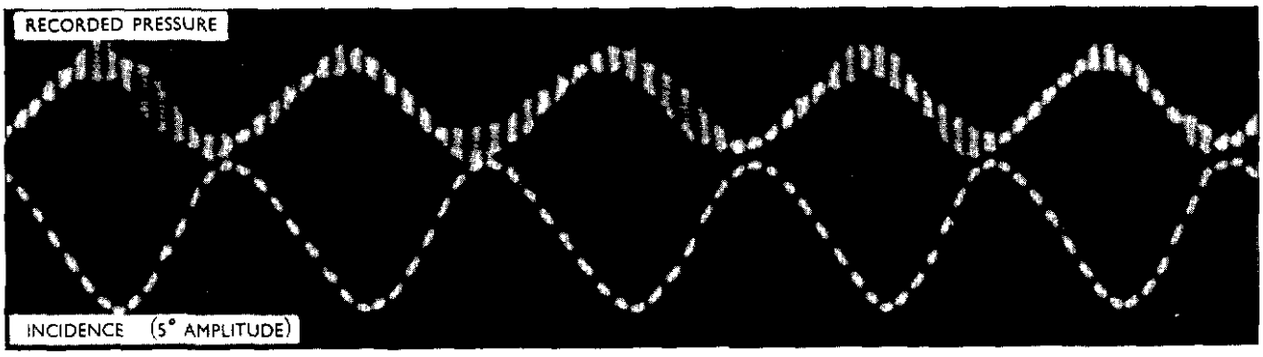

FORCING FREQUENCY = 16·2 c p s TIME BASE 250 c p s M = 1·9

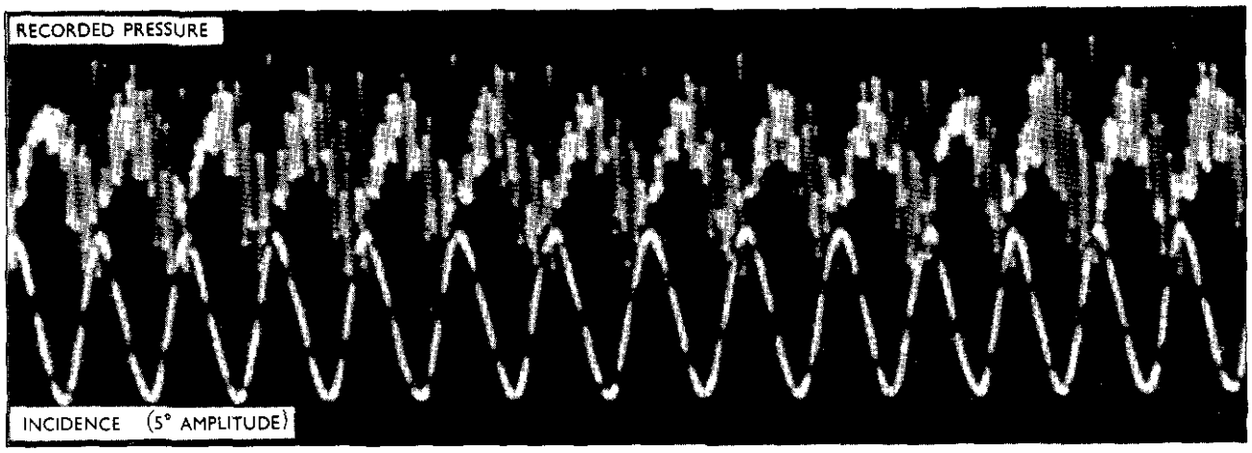

FORCING FREQUENCY = 45 c p s TIME BASE 250 c p s M = 1·4

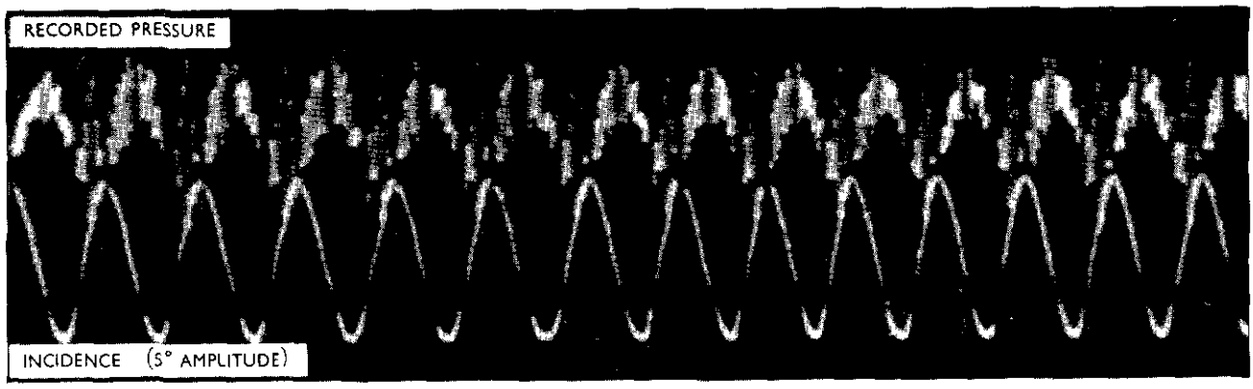

FORCING FREQUENCY = 45 c p s TIME BASE 135 c p s M = 1·9

NOTE - Displacements are shown opposite in sense for clarity

FIG 19 STEADY STATE PRESSURE RESPONSE AT FAST PROGRAMME SPEEDS (CAPACITY TYPE PICK-UP)

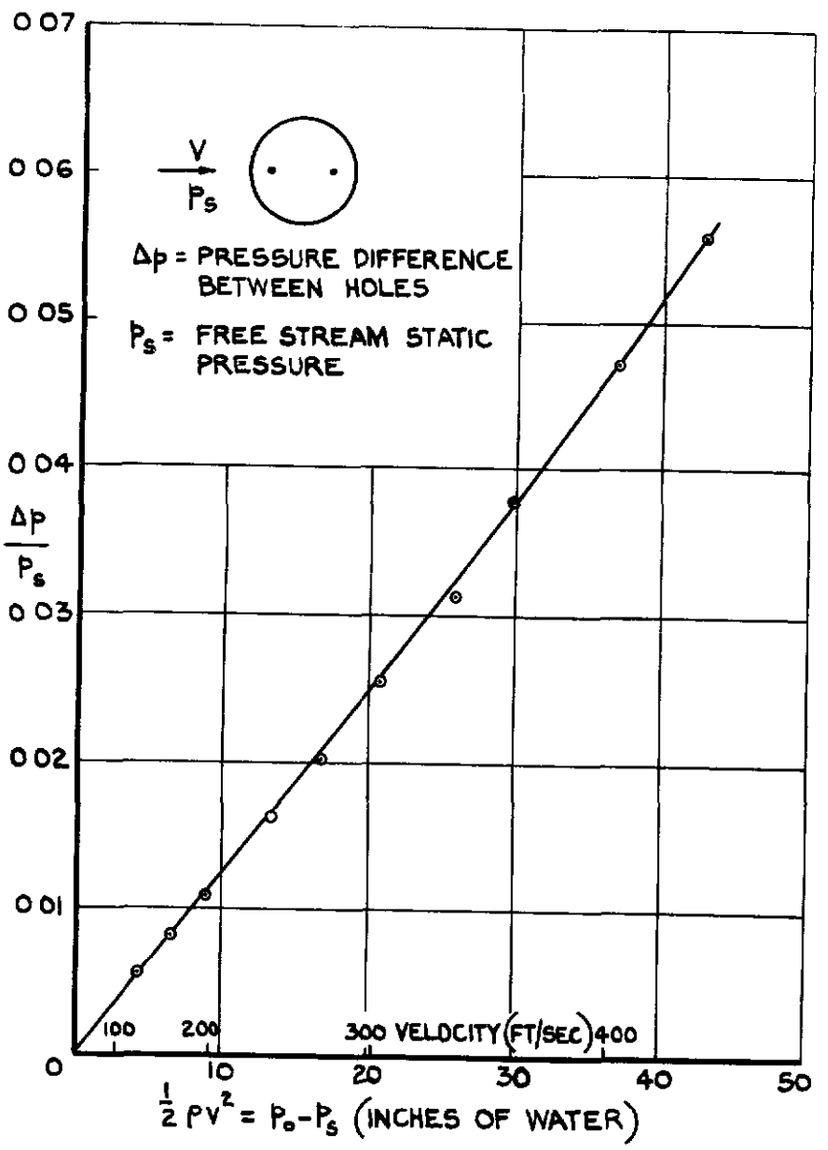

FIG.20. PRESSURE DIFFERENCE DUE TO AN INDEPENDENT (SUBSONIC) CROSS FLOW VELOCITY.

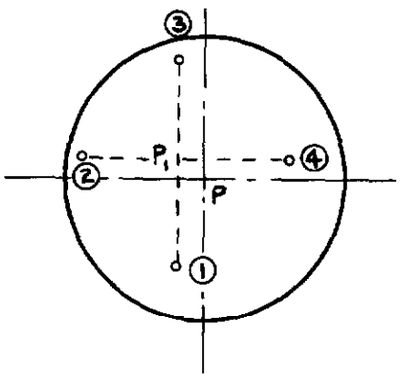

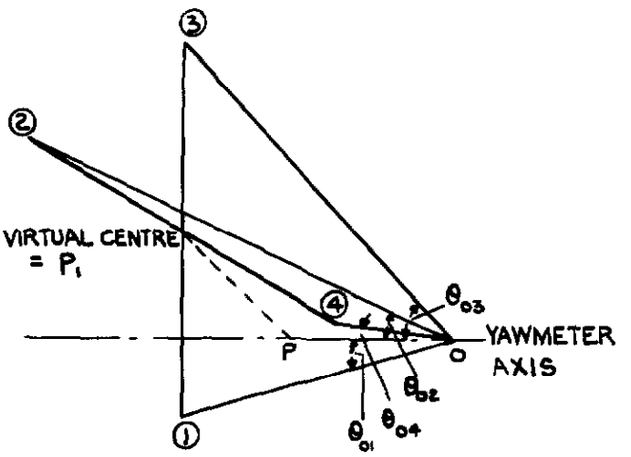

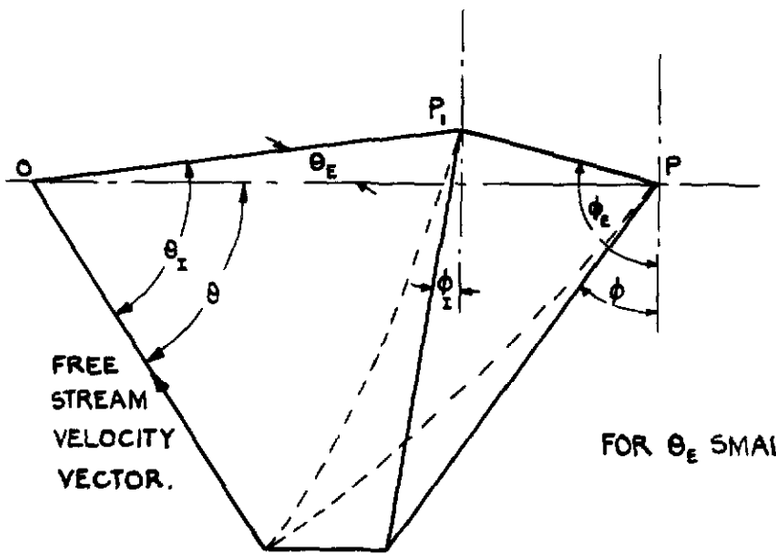

FOR θ_E SMALL, $OP_1 \doteq OP$

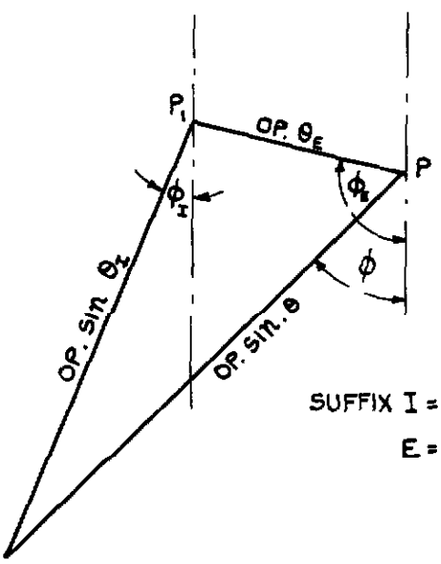

SUFFIX I = INDICATED BY INSTRUMENT
E = MANUFACTURING ERROR.

FIG.21. GEOMETRIC RELATIONS BETWEEN INDICATED AND TRUE INCIDENCE AND ROLL ANGLE.

C.P. No. 414
(20,474)
A.R.C. Technical Report

Published by
HER MAJESTY'S STATIONERY OFFICE

To be purchased from
York House, Kingsway, London w c 2
423 Oxford Street, London w 1
13A Castle Street, Edinburgh 2
109 St. Mary Street, Cardiff
39 King Street, Manchester 2
Tower Lane, Bristol 1
2 Edmund Street, Birmingham 3
80 Chichester Street, Belfast
or through any bookseller

Printed in Great Britain

S.O. Code No. 23-9011-14

C.P. No. 414